Eur. Phys. J. C 56, 125–146 (2008)
DOI 10.1140/epjc/s10052-008-0625-3

THE EUROPEAN PHYSICAL JOURNAL C

Regular Article – Theoretical Physics

Lepton flavor violating leptonic and semileptonic decays of charged leptons in the minimal supersymmetric standard model

T. Fukuyama[1,a], A. Ilakovac[2,b], T. Kikuchi[3,4,c]

[1] Department of Physics, Ritsumeikan University, Kusatsu, Shiga, 525-8577 Japan
[2] Department of Physics, University of Zagreb, P.O. Box 331, Bijenička cesta 32, 10002 Zagreb, Croatia
[3] Theory Division, KEK, Oho 1-1, Tsukuba, Ibaraki, 305-0801, Japan
[4] Department of Physics, Oklahoma State University, Stillwater, OK 74078, USA

Received: 21 February 2008 /
Published online: 25 June 2008 –

Abstract. We consider the leptonic and semileptonic (SL) lepton-flavor violating (LFV) decays of the charged leptons in the minimal supersymmetric standard model (MSSM) with right-handed neutrinos. The parameters of the MSSM model are determined in the framework of the minimal supersymmetric SO(10) GUT model assuming the minimal supergravity model of supersymmetry breaking. The free parameters of the model are constrained adopting the WMAP cold dark matter constraint and adjusting the neutrino oscillation data. So constrained, the SO(10) GUT model gives a definite prediction for the Dirac-neutrino Yukawa matrix, which induces all LFV effects in the MSSM model through renormalization group equations of soft SUSY breaking parameters. A very detailed numerical analysis has been made to define numerically all MSSM parameters necessary for the evaluation of the LFV amplitudes. The basic LFV amplitudes in MSSM were rederived and improved. The formalism for the evaluation of all SL LFV amplitudes is given. Numerical results for dominant SL LFV branching ratios, the anomalous magnetic moment of the muon and the $\ell \to \ell'\gamma$ branching ratios are given.

1 Introduction

The discovery of neutrino oscillations [1] is the first experimental evidence of physics beyond the standard model (SM) of the electroweak interactions. In SM, neutrinos are massless purely left-handed particles, so there is no leptonic analogy of the Cabibbo–Kobayashi–Maskawa (CKM) matrix. The neutrino oscillation experiments proved that the neutrinos do mix and that they do have mass. The mixing matrix in the lepton sector, the Maki–Nakagawa–Sakata (MNS) matrix [2] has a bi-large mixing structure [3–5], indicating that the source of the lepton-flavor mixing is different from the corresponding mixing in the quark sector. The lepton-flavor mixing observed in neutrino oscillations is the first confirmation that the lepton flavor is not a conserved quantity. Therefore, experimental observation of the other lepton-flavor violating (LFV) processes is naturally expected. The theoretical study of such processes has a long history before the observation of neutrino oscillations. The model-independent study of the operators using SM fields [6–8] shows that there are no LFV operators of dimension less or equal to four. There is one dimension five LFV operator that induces neutrino oscillations. The LFV decays can be induced only with the operators of dimension six or more. As new physics is expected to appear at the scale much larger than the electroweak scale $\sim 246\,\mathrm{GeV}$, the LFV decay effects are expected to be much more suppressed than the neutrino oscillation effects. A model-independent study of the LFV processes gives the limits on LFV which every model has to satisfy. A model-dependent analysis is determined by the structure of the model but is much more predictive than the corresponding model-independent analysis. Therefore, both approaches are indispensable for a theoretical study of LFV. Although the leptonic LFV processes have been studied extensively both in a model-independent way and using various models [9–40, 42, 43][1], the semileptonic (SL) LFV processes have been studied only in a few models [44–50].

Supersymmetric (SUSY) models have much nicer theoretical properties than their non-SUSY counterparts. For example, quadratically-divergent contributions to the Higgs boson mass from heavy (e.g. GUT scale) particles

[a] e-mail: fukuyama@se.ritsumei.ac.jp
[b] e-mail: ailakov@rosalind.phy.hr
[c] e-mail: tatsuru@post.kek.jp

[1] For a recent review, see, for example, [41] and references therein.

cancel with its SUSY partners, and as a result the gauge-hierarchy problem is much better resolved. The supersymmetrization of SM cannot be done without additional assumptions. For instance, in the supersymmetric version of SM there are dimension-four operators violating both lepton number ($\not{L}$) and baryon number ($\not{B}$), leading to very fast proton decay [52–57]. That led us to the introduction of a discrete $\mathbb{Z}_2$ symmetry, the so-called R-parity [51–57] to forbid such undesirable terms. SUSY breaking has also to be done in such a way as not to induce too large flavor-violation effects. There are few successful SUSY-breaking mediation mechanisms, such as gravity mediation [58–60], gauge mediation [61, 62], anomaly mediation [63, 64], gaugino mediation [65–67], radion mediation [68], etc. The best established among them is the minimal supergravity model (mSUGRA) [58–60], which assumes that SUSY breaking occurs in the hidden sector at a very high scale, which communicates with the visible sector (containing SM) with flavor-blind gravitational interactions. The induced soft SUSY-breaking mass terms are required to be universal at the SUSY-breaking mediation scale (say, the (reduced) Planck scale), and are therefore flavor-diagonal. The magnitude of the soft SUSY-breaking mass terms obtained is in such a range that they may induce potentially observable consequences in the visible sector. The renormalization group (RG) flow from the (reduced) Planck scale to the mass scale of the right-handed neutrinos induces the flavor non-diagonal terms in the SUSY soft-breaking terms for the sleptons, through the flavor non-diagonal Dirac-neutrino Yukawa matrices they contain [69]. They can lead to considerable LFV effects, which, depending on the model parameters may be in the range of the forthcoming LFV experiments [70–73].

In this paper, we assume MSSM with three right-handed neutrinos as the low-energy effective theory below the GUT scale. In such a framework, the neutrino oscillation data suggest the existence of very massive right-handed neutrinos which give rise to small left-handed neutrino masses through the see-saw mechanism [74–76]. In SO(10) models, the required right-handed neutrinos may naturally be embedded into the common multiplet together with the SM particles for each generation. In this paper, the minimal renormalizable SUSY SO(10) model [77–87] will be taken as a theoretical starting frame. One of the advantageous points of this model is the automatically conserved R-parity defined as $R = (-1)^{3(B-L)+2S}$ [51, 54–57, 103], where S represents the spin of a field. Namely, the SO(10) model discussed here spontaneously breaks the gauged B–L symmetry by two units, leading to automatic R-parity conservation. The breaking of the SO(10) group to the SM gauge group, $\mathrm{SU}(3)_C \times \mathrm{SU}(2)_\mathrm{L} \times \mathrm{U}(1)_Y$ [88–90] and its phenomenological consequences [43, 91, 92] has already been discussed in our previous publications.

The main goal of this paper is an analysis of neutrinoless SL LFV decays of charged leptons within the MSSM model, where the parameters are obtained from the underlying SO(10) model. At the same time, we intend to see how the previous phenomenological analyses constrain the LFV parameters. The paper consists basically of three parts, which are given in three sections. In Sect. 2, we give the MSSM form factors comprised in the LFV amplitudes at the quark–lepton level. We rederive these form factors, because some of them were not derived completely in the previous literature. In Sect. 3, the charged-lepton SL LFV amplitudes at the lepton–meson level are derived using a simple hadronization procedure for the quark currents. The branching ratios corresponding to these amplitudes are also given. In Sect. 4, the minimal renormalizable SUSY SO(10) model is described. Constraining the free SO(10) model parameters by adjusting the neutrino oscillation data with corresponding theoretical quantities at the electroweak scale, the Dirac-neutrino Yukawa matrix is fixed. With the SO(10) model parameters and Dirac-neutrino Yukawa couplings thus fixed, the parameters of the MSSM model at the electroweak scale are derived, too. Using the MSSM model parameters thus derived, a numerical estimate for the SL LFV processes is performed. The last section is devoted to a summary. In Appendix A, we give our notation for the neutralino, chargino and sfermion mass matrices. The MSSM Lagrangian for the fermion–sfermion–(gaugino, Higgsino) interaction and the trilinear interactions with the Z boson are given in Appendices B and C, respectively. In Appendix D, we present the loop functions needed to evaluate the SL LFV processes. The quark content of the meson states, essential for the hadronization of quark currents, is listed in Appendix E, together with the constants that define the hadronized quark current in the γ-penguin and Z-boson-penguin amplitude.

2 Effective lagrangian for LFV interactions

2.1 Sources for LFV interactions

Even though the soft SUSY-breaking parameters are flavor blind at the scale of the SUSY-breaking mediation, the LFV interactions in the model can induce the LFV sources at low energy through renormalization effects [69, 70]. In the following analysis, we assume the mSUGRA scenario [58–60] as the SUSY-breaking mediation mechanism. At the scale of the SUSY-breaking mediation, which is taken to coincide with the GUT scale, we impose the boundary conditions on the soft SUSY-breaking parameters, which are characterized by five parameters [93, 94]: m_0, $M_{1/2}$, A_0, B and μ. Here, m_0 is the universal scalar mass, $M_{1/2}$ is the universal gaugino mass, and A_0 is the universal coefficient of the trilinear couplings. The parameters in the Higgs potential, B and μ, are determined at the electroweak scale so that the Higgs doublets obtain the correct electroweak symmetry-breaking VEVs through the radiative breaking scenario [94–98]. The soft SUSY-breaking parameters at low energies are obtained through their RGE evolution from their boundary-condition values at the GUT scale to the electroweak scale.

Although the SUSY-breaking mediation scale is normally taken to be the (reduced) Planck scale [70, 98, 99] or the string scale ($\sim 10^{18}$ GeV), in the following calcula-

tions we impose the boundary conditions at the GUT scale ($\sim 10^{16}$ GeV). This ansatz is the same as the one in the so-called constrained MSSM (CMSSM) [94].

The effective theory which we analyze below the GUT scale is MSSM with right-handed neutrinos. The superpotential is given by [70]

$$W_{\rm Y} = Y_u^{ij}\,(u_{\rm R}^c)_i\,q_j H_u + Y_d^{ij}\,(d_{\rm R}^c)_i\,q_j H_d + Y_\nu^{ij}\,(\nu_{\rm R}^c)_i\,\ell_j H_u + Y_e^{ij}\,(e_{\rm R}^c)_i\,\ell_j H_d + \frac{1}{2}M_{{\rm R}_{ij}}\,(\nu_{\rm R}^c)_i\,(\nu_{\rm R}^c)_j + \mu H_d H_u\,, \tag{1}$$

where the indices i, j run over three generations, H_u and H_d denote the up-type and down-type MSSM Higgs doublets, respectively, and $M_{{\rm R}_{ij}}$ is the heavy right-handed Majorana neutrino mass matrix. We work in the basis in which the charged-lepton Yukawa matrix Y_e and the mass matrix $M_{{\rm R}_{ij}}$ are real, positive and diagonal matrices [70]: $Y_e^{ij} = Y_{e_i}\delta_{ij}$ and $M_{{\rm R}_{ij}} = {\rm diag}(M_{{\rm R}_1}, M_{{\rm R}_2}, M_{{\rm R}_3})$. Thus, LFV originates from the off-diagonal components of the Dirac-neutrino Yukawa coupling matrix Y_ν. The soft SUSY-breaking terms are [70]

$$\begin{aligned}-\mathcal{L}_{\rm soft} = {}& \tilde{q}_i^\dagger\left(m_{\tilde{q}}^2\right)_{ij}\tilde{q}_j + \tilde{u}_{{\rm R}i}^\dagger\left(m_{\tilde{u}}^2\right)_{ij}\tilde{u}_{{\rm R}j} + \tilde{d}_{{\rm R}i}^\dagger\left(m_{\tilde{d}}^2\right)_{ij}\tilde{d}_{{\rm R}j} \\ & + \tilde{\ell}_i^\dagger\left(m_{\tilde{\ell}}^2\right)_{ij}\tilde{\ell}_j + \tilde{\nu}_{{\rm R}i}^\dagger\left(m_{\tilde{\nu}}^2\right)_{ij}\tilde{\nu}_{{\rm R}j} + \tilde{e}_{{\rm R}i}^\dagger\left(m_{\tilde{e}}^2\right)_{ij}\tilde{e}_{{\rm R}j} \\ & + m_{H_u}^2 H_u^\dagger H_u + m_{H_d}^2 H_d^\dagger H_d \\ & + \left(B\mu H_d H_u + \frac{1}{2}B_\nu M_{{\rm R}_{ij}}\tilde{\nu}_{{\rm R}i}^\dagger\tilde{\nu}_{{\rm R}j} + {\rm h.c.}\right) \\ & + \left(A_u^{ij}\tilde{u}_{{\rm R}i}^\dagger\tilde{q}_j H_u + A_d^{ij}\tilde{d}_{{\rm R}i}^\dagger\tilde{q}_j H_d + {\rm h.c.}\right) \\ & + \left(A_\nu^{ij}\tilde{\nu}_{{\rm R}i}^\dagger\tilde{\ell}_j H_u + A_e^{ij}\tilde{e}_{{\rm R}i}^\dagger\tilde{\ell}_j H_d + {\rm h.c.}\right) \\ & + \left(\frac{1}{2}M_1\tilde{B}\tilde{B} + \frac{1}{2}M_2\tilde{W}^a\tilde{W}^a + \frac{1}{2}M_3\tilde{G}^a\tilde{G}^a + {\rm h.c.}\right).\end{aligned} \tag{2}$$

The universal boundary conditions at the GUT scale (see e.g. [70, 100–102]) read

$$\begin{aligned}\left(m_{\tilde{q}}^2\right)_{ij} &= \left(m_{\tilde{u}}^2\right)_{ij} = \left(m_{\tilde{d}}^2\right)_{ij} = m_0^2\delta_{ij}\,, \\ \left(m_{\tilde{\ell}}^2\right)_{ij} &= \left(m_{\tilde{\nu}}^2\right)_{ij} = \left(m_{\tilde{e}}^2\right)_{ij} = m_0^2\delta_{ij}\,, \\ m_{H_u}^2 &= m_{H_d}^2 = m_0^2\,, \\ A_u^{ij} &= A_0 Y_u^{ij}\,, \quad A_d^{ij} = A_0 Y_d^{ij}\,, \\ A_\nu^{ij} &= A_0 Y_\nu^{ij}\,, \quad A_e^{ij} = A_0 Y_e^{ij}\,, \\ M_1 &= M_2 = M_3 = M_{1/2}\,.\end{aligned} \tag{3}$$

The soft SUSY-breaking parameters are evolved to the electroweak scale according to their RGEs given in [103, 104]. The μ parameter and the B parameter are determined at the electroweak scale minimizing the Higgs potential [94],

$$\begin{aligned}|\mu|^2 &= \frac{m_{H_d}^2 - m_{H_u}^2\tan^2\beta}{\tan^2\beta - 1} - \frac{1}{2}M_Z^2\,, \\ B\mu &= -\frac{1}{2}\left(m_{H_d}^2 + m_{H_u}^2 + 2|\mu|^2\right)\sin 2\beta\left(= \frac{1}{2}m_A^2\sin 2\beta\right).\end{aligned} \tag{4}$$

The off-diagonal components of the matrices of the soft diagonal SUSY parameters, such as $\left(m_{\tilde{\ell}}^2\right)_{ij}$ and A_e^{ij}, are sources of LFV. They are induced through the Dirac-neutrino Yukawa terms in the RGEs [70, 104], such as

$$\begin{aligned}&\mu\frac{\rm d}{{\rm d}\mu}\left(m_{\tilde{\ell}}^2\right)_{ij} = \\ &\mu\frac{\rm d}{{\rm d}\mu}\left(m_{\tilde{\ell}}^2\right)_{ij}\Big|_{\rm MSSM} + \frac{1}{16\pi^2}\big(m_{\tilde{\ell}}^2 Y_\nu^\dagger Y_\nu + Y_\nu^\dagger Y_\nu m_{\tilde{\ell}}^2 \\ &+ 2Y_\nu^\dagger m_{\tilde{\nu}}^2 Y_\nu + 2m_{H_u}^2 Y_\nu^\dagger Y_\nu + 2A_\nu^\dagger A_\nu\big)_{ij}\,.\end{aligned} \tag{5}$$

The first term on the right-hand side of (5) denotes the flavor-diagonal MSSM term. In the leading-logarithmic approximation, the off-diagonal components ($i \neq j$) of the left-handed slepton mass matrix read [43, 70, 104]

$$\left(\Delta m_{\tilde{\ell}}^2\right)_{ij} \sim -\frac{3m_0^2 + A_0^2}{8\pi^2}\left(Y_\nu^\dagger L Y_\nu\right)_{ij}\,. \tag{6}$$

Distinct thresholds for the right-handed Majorana neutrinos are taken into account by the matrix

$$L_{ij} = \log\left(\frac{M_G}{M_{{\rm R}_i}}\right)\delta_{ij}\,.$$

It is obvious that the Dirac-neutrino Yukawa coupling matrix plays a crucial role in calculations of the LFV processes.

2.2 Effective Lagrangian in terms of quark fields and LFV form factors

In any model containing the standard model as the low-energy effective theory in the lowest order of perturbation theory, an effective Lagrangian for the SL LFV decays of a lepton contains only three terms: the photon-penguin, the Z-boson-penguin and the box term,

$${\rm i}\mathcal{L}_{\rm eff}\left(\ell_i \to \ell_j + \bar{q} + q'\right) = {\rm i}\mathcal{L}_{\rm eff}^\gamma + {\rm i}\mathcal{L}_{\rm eff}^Z + {\rm i}\mathcal{L}_{\rm eff}^{\rm box}\,. \tag{7}$$

These terms have the following generic structure:

$$\begin{aligned}{\rm i}\mathcal{L}_{\rm eff}^\gamma(x) = {}& -{\rm i}e^2\int {\rm d}^4 y\,\bar{\ell}_j(x)\Big[\left(-\partial_x^2\gamma_\mu + \not{\partial}_x\partial_{x\mu}\right)D(x-y) \\ & \times\left(\mathcal{P}_{1\gamma}^{\rm L}P_{\rm L} + \mathcal{P}_{1\gamma}^{R}P_{\rm R}\right) \\ & + \sigma_{\mu\nu}\partial_x^\nu D(x-y)\left(\mathcal{P}_{2\gamma}^{\rm L}P_{\rm L} + \mathcal{P}_{2\gamma}^{\rm R}P_{\rm R}\right)\Big]\ell_i(x) \\ & \times\sum_{q=u,d,s} Q_q\bar{q}(y)\gamma^\mu q(y)\,,\end{aligned} \tag{8}$$

$$\begin{aligned}{\rm i}\mathcal{L}_{\rm eff}^Z(x) = {}& {\rm i}\frac{g^2}{m_Z^2 c_{\rm W}^2}\bar{\ell}_j(x)\gamma_\mu(\mathcal{P}_Z^{\rm L}P_{\rm L} + \mathcal{P}_Z^{\rm R}P_{\rm R})\ell_i(x) \\ & \times\sum_{q=u,d,s}\bar{q}\left(I_{3q} - 2Q_q s_{\rm W}^2\right)\gamma^\mu - I_{3q}\gamma^\mu\gamma_5)q(x)\,,\end{aligned} \tag{9}$$

$$
\begin{aligned}
\mathrm{i}\mathcal{L}_{\mathrm{eff}}^{\mathrm{box}} = \mathrm{i} \sum_{\bar{q}_a q_b = \bar{u}u, \bar{d}d, \bar{s}s, \bar{d}s, \bar{s}d} \Big[& \mathcal{B}^{\mathrm{L}}_{1\bar{q}_a q_b} \left(\bar{\ell}_j \gamma^\mu P_{\mathrm{L}} \ell_i\right) \left(\bar{q}_a \gamma_\mu P_{\mathrm{L}} q_b\right) \\
& + \mathcal{B}^{\mathrm{R}}_{1\bar{q}_a q_b} \left(\bar{\ell}_j \gamma^\mu P_{\mathrm{R}} \ell_i\right) \left(\bar{q}_a \gamma_\mu P_{\mathrm{R}} q_b\right) \\
& + \mathcal{B}^{\mathrm{L}}_{2\bar{q}_a q_b} \left(\bar{\ell}_j \gamma^\mu P_{\mathrm{L}} \ell_i\right) \left(\bar{q}_a \gamma_\mu P_{\mathrm{R}} q_b\right) \\
& + \mathcal{B}^{\mathrm{R}}_{2\bar{q}_a q_b} \left(\bar{\ell}_j \gamma^\mu P_{\mathrm{R}} \ell_i\right) \left(\bar{q}_a \gamma_\mu P_{\mathrm{L}} q_b\right) \\
& + \mathcal{B}^{\mathrm{L}}_{3\bar{q}_a q_b} (\bar{\ell}_j P_{\mathrm{L}} \ell_i)(\bar{q}_a P_{\mathrm{L}} q_b) \\
& + \mathcal{B}^{\mathrm{R}}_{3\bar{q}_a q_b} (\bar{\ell}_j P_{\mathrm{R}} \ell_i)(\bar{q}_a P_{\mathrm{R}} q_b) \\
& + \bar{\mathcal{B}}^{\mathrm{L}}_{3\bar{q}_a q_b} (\bar{\ell}_j P_{\mathrm{L}} \ell_i)(\bar{q}_a P_{\mathrm{R}} q_b) \\
& + \bar{\mathcal{B}}^{\mathrm{R}}_{3\bar{q}_a q_b} (\bar{\ell}_j P_{\mathrm{R}} \ell_i)(\bar{q}_a P_{\mathrm{L}} q_b) \\
& + \mathcal{B}^{\mathrm{L}}_{4\bar{q}_a q_b} (\bar{\ell}_j \sigma_{\mu\nu} P_{\mathrm{L}} \ell_i) \left(\bar{q}_a \sigma^{\mu\nu} P_{\mathrm{R}} q_b\right) \\
& + \mathcal{B}^{\mathrm{R}}_{4\bar{q}_a q_b} (\bar{\ell}_j \sigma_{\mu\nu} P_{\mathrm{R}} \ell_i) \left(\bar{q}_a \sigma^{\mu\nu} P_{\mathrm{L}} q_b\right) \Big] , \qquad (10)
\end{aligned}
$$

where $s_{\mathrm{W}} = \sin\theta_{\mathrm{W}}$ and $c_{\mathrm{W}} = \cos\theta_{\mathrm{W}}$, Q_q is the quark charge in units of electromagnetic charge e, and I_{3q} is the weak quark isospin; g is the weak coupling constant; $P_{\mathrm{R,L}} = \frac{1}{2}(1 \pm \gamma_5)$; $D(x-y)$ is the Green function for the massless scalar particle, contained in the photon propagator. The structure of the photon-penguin term in the effective Lagrangian is a consequence of the gauge invariance. Especially, the first term must contain $\partial_x \partial_{x\mu}$, which was neglected in [70]. The information of the model under consideration is contained in the form factors $\mathcal{P}^{\mathrm{L,R}}_{a\gamma}$, $a = 1, 2$, $\mathcal{P}^{\mathrm{L,R}}_{Z}$, $\bar{\mathcal{B}}^{\mathrm{L}}_{3\bar{q}_a q_b}$, and $\mathcal{B}^{\mathrm{L,R}}_{a\bar{q}_a q_b}$, $a = 1, 2, 3, 4$. In the following three subsections, these form factors are given for the MSSM.

2.2.1 The photon-penguin form factors

The amplitude for $\ell_i \to \ell_j \gamma^*$ for an off-mass-shell photon process is obtained from the corresponding part of the effective Lagrangian neglecting the quark current and the photon propagator,

$$
\begin{aligned}
\mathcal{M}_\mu{}^\gamma = \mathrm{i}T^\gamma_\mu = -e\overline{u}_{\ell_j} \Big[& \left(q^2 \gamma_\mu - q_\mu \not{q}\right) \left(\mathcal{P}^{\mathrm{L}}_{1\gamma} P_{\mathrm{L}} + \mathcal{P}^{\mathrm{R}}_{1\gamma} P_{\mathrm{R}}\right) \\
& + \mathrm{i}\sigma_{\mu\nu} q^\nu \left(\mathcal{P}^{\mathrm{L}}_{2\gamma} P_{\mathrm{L}} + \mathcal{P}^{\mathrm{R}}_{2\gamma} P_{\mathrm{R}}\right) \Big] u_{\ell_i} . \qquad (11)
\end{aligned}
$$

The amplitude is written without photon polarization vector.

In the MSSM the photon-penguin amplitude has two contributions, a chargino and a neutralino contribution (see e.g. [70]). This is reflected in the structure of the form factors,

$$
\mathcal{P}^{\mathrm{L,R}}_{a\gamma} = \mathcal{P}^{(C)\mathrm{L,R}}_{a\gamma} + \mathcal{P}^{(N)\mathrm{L,R}}_{a\gamma} , \quad a = 1, 2 , \qquad (12)
$$

with the C and N superscripts denoting the chargino and neutralino part of a form factor.

Because of gauge invariance, the zeroth-order term and the first-order term in the Taylor expansion in the momenta and masses of the incoming and outgoing particles are equal to zero. Here, the second-order term in the Taylor expansion is presented, and higher-order terms are neglected.

The neutralino contributions are

$$
\begin{aligned}
\mathcal{P}^{(N)\mathrm{L}}_{1\gamma} = & \frac{\mathrm{i}}{576\pi^2} N^{\mathrm{R}(e)}_{jAX} N^{\mathrm{R}(e)*}_{iAX} \frac{1}{m^2_{\tilde{e}_X}} \\
& \times \frac{11(x^0_{AX})^3 - 18(x^0_{AX})^2 + 9(x^0_{AX}) - 2 - 6(x^0_{AX})^3 \ln(x^0_{AX})}{(1 - x^0_{AX})^4} \qquad (13)
\end{aligned}
$$

$$
\mathcal{P}^{(N)\mathrm{R}}_{1\gamma} = \mathcal{P}^{(N)\mathrm{L}}_{1\gamma}|_{\mathrm{L}\leftrightarrow\mathrm{R}} , \qquad (14)
$$

$$
\begin{aligned}
\mathcal{P}^{(N)\mathrm{L}}_{2\gamma} = & \frac{i}{32\pi^2} \Bigg[N^{\mathrm{R}(e)}_{jAX} N^{\mathrm{R}(e)*}_{iAX} (-1) m_j \frac{1}{m^2_{\tilde{e}_X}} \\
& \times \frac{2(x^0_{AX})^3 + 3(x^0_{AX})^2 - 6(x^0_{AX}) + 1 - 6(x^0_{AX})^2 \ln(x^0_{AX})}{6(1 - x^0_{AX})^4} \\
& + N^{\mathrm{L}(e)}_{jAX} N^{\mathrm{L}(e)*}_{iAX} (-1) m_i \frac{1}{m^2_{\tilde{e}_X}} \\
& \times \frac{2(x^0_{AX})^3 + 3(x^0_{AX})^2 - 6(x^0_{AX}) + 1 - 6(x^0_{AX})^2 \ln(x^0_{AX})}{6(1 - x^0_{AX})^4} \\
& + N^{\mathrm{L}(e)}_{jAX} N^{\mathrm{R}(e)*}_{iAX} (-1) m_{\tilde{\chi}^0_A} \frac{1}{m^2_{\tilde{e}_X}} \\
& \times \frac{-(x^0_{AX})^2 + 1 + 2(x^0_{AX}) \ln(x^0_{AX})}{(1 - x^0_{AX})^3} \Bigg] , \qquad (15)
\end{aligned}
$$

$$
\mathcal{P}^{(N)\mathrm{R}}_{2\gamma} = \mathcal{P}^{(N)\mathrm{L}}_{2\gamma}|_{\mathrm{L}\leftrightarrow\mathrm{R}} , \qquad (16)
$$

where $x^0_{AX} = M^2_{\tilde{\chi}^0_A} / m^2_{\tilde{e}_X}$. The chargino contributions are given by

$$
\begin{aligned}
\mathcal{P}^{(C)\mathrm{L}}_{1\gamma} = & \frac{\mathrm{i}}{576\pi^2} C^{\mathrm{R}(e)}_{jAX} C^{\mathrm{R}(e)*}_{iAX} \frac{1}{m^2_{\tilde{\nu}_X}} \\
& \times \big(16 - 45(x^-_{AX}) + 36(x^-_{AX})^2 - 7(x^-_{AX})^3 \\
& + 6(2 - 3(x^-_{AX})) \ln(x^-_{AX})\big) \frac{1}{(1 - x^-_{AX})^4} , \qquad (17)
\end{aligned}
$$

$$
\mathcal{P}^{(C)\mathrm{R}}_{1\gamma} = \mathcal{P}^{(C)\mathrm{L}}_{1\gamma}|_{\mathrm{L}\leftrightarrow\mathrm{R}} , \qquad (18)
$$

$$
\begin{aligned}
\mathcal{P}^{(C)\mathrm{L}}_{2\gamma} = & \frac{i}{32\pi^2} \Bigg[C^{\mathrm{R}(e)}_{jAX} C^{\mathrm{R}(e)*}_{iAX} m_j \frac{1}{m^2_{\tilde{\nu}_X}} \\
& \times \frac{2 + 3(x^-_{AX}) - 6(x^-_{AX})^2 + (x^-_{AX})^3 + 6(x^-_{AX}) \ln(x^-_{AX})}{6(1 - x^-_{AX})^4} \\
& + C^{\mathrm{L}(e)}_{jAX} C^{\mathrm{L}(e)*}_{iAX} m_i \frac{1}{m^2_{\tilde{\nu}_X}} \\
& \times \frac{2 + 3(x^-_{AX}) - 6(x^-_{AX})^2 + (x^-_{AX})^3 + 6(x^-_{AX}) \ln(x^-_{AX})}{6(1 - x^-_{AX})^4} \\
& + C^{\mathrm{L}(e)}_{jAX} C^{\mathrm{R}(e)*}_{iAX} m_{\tilde{\chi}^-_A} \\
& \times \frac{1}{m^2_{\tilde{\nu}_X}} \frac{-3 + 4(x^-_{AX}) - (x^-_{AX})^2 - 2\ln(x^-_{AX})}{(1 - x^-_{AX})^3} \Bigg] , \qquad (19)
\end{aligned}
$$

$$
\mathcal{P}^{(C)\mathrm{R}}_{2\gamma} = \mathcal{P}^{(C)\mathrm{L}}_{2\gamma}|_{\mathrm{L}\leftrightarrow\mathrm{R}} , \qquad (20)
$$

where $x^-_{AX} = M^2_{\tilde{\chi}^-_A} / m^2_{\tilde{\nu}_X}$. To make the comparison with the results of [70] easy, the form factor contributions are written in the same way, including the explicit expressions for the loop functions. Both the chargino and neutralino

part of the form factors agree with the corresponding form factors in [70] if the terms proportional to the mass of the lighter mesons m_j are neglected. Nevertheless, these terms cannot be neglected, because the constants $N_{jAX}^{\mathrm{L,R}(e)}$ and $C_{jAX}^{\mathrm{L,R}(e)}$ (see Appendix B) also depend on the lepton masses in such a way that in some cases the term proportional to m_j is larger than the term proportional to the mass of the decaying lepton m_i.

2.2.2 The Z-penguin form factors

The amplitude for the off-mass-shell $\ell_i \to \ell_j Z^*$ amplitude reads

$$\mathcal{M}_\mu^Z = \frac{\mathrm{i}}{(4\pi)^2} g \overline{u}_{\ell_j} \Big[\gamma_\mu P_\mathrm{L} \left(\mathcal{P}_Z^{(C)\mathrm{L}} + \mathcal{P}_Z^{(N)\mathrm{L}} \right) + \gamma_\mu P_\mathrm{R} \left(\mathcal{P}_Z^{(C)\mathrm{R}} + \mathcal{P}_Z^{(N)\mathrm{R}} \right) \Big] u_{\ell_i} \,, \tag{21}$$

where $\mathcal{P}_Z^{(C)\mathrm{L,R}}$ and $\mathcal{P}_Z^{(N)\mathrm{L,R}}$ are the chargino and neutralino parts of the total form factors, $\mathcal{P}_Z^{\mathrm{L,R}}$. The expressions for these form factors are

$$\begin{aligned}
&\mathcal{P}_Z^{(C)\mathrm{L}} = \\
&C_{jBX}^{\mathrm{R}(e)} C_{iAX}^{\mathrm{R}(e)*} \Big[E_{BA}^{\mathrm{L}(\tilde{\chi}^-)} m_{\tilde{\chi}_B^-} m_{\tilde{\chi}_A^-} F_1 \left(m_{\tilde{\nu}_X}^2, m_{\tilde{\chi}_A^-}^2, m_{\tilde{\chi}_B^-}^2 \right) \\
&- 2 E_{BA}^{\mathrm{R}(\tilde{\chi}^-)} F_2 \left(m_{\tilde{\nu}_X}^2, m_{\tilde{\chi}_A^-}^2, m_{\tilde{\chi}_B^-}^2 \right) \\
&+ \delta_{AB} G_{Ze}^\mathrm{L} f_1 \left(m_{\tilde{\nu}_X}^2, m_{\tilde{\chi}_A^-}^2 \right) \Big] \\
&+ \left\{ C_{jBX}^{\mathrm{R}(e)} E_{BA}^{\mathrm{L}(\tilde{\chi}^-)} C_{iAX}^{\mathrm{L}(e)*} \left[-2 F_2 \left(m_{\tilde{\nu}_X}^2, m_{\tilde{\chi}_A^-}^2, m_{\tilde{\chi}_B^-}^2 \right) \right] \right\},
\end{aligned} \tag{22}$$

$$\begin{aligned}
&\mathcal{P}_Z^{(N)\mathrm{L}} = \\
&N_{jAY}^{\mathrm{R}(e)} N_{iAX}^{\mathrm{R}(e)*} \Big[-2 D_{YX}^{(\tilde{e})} F_2 \left(m_{\tilde{\chi}_A^0}^2, m_{\tilde{e}_X}^2, m_{\tilde{e}_Y}^2 \right) \\
&+ \delta_{YX} G_{Ze}^\mathrm{L} f_2 \left(m_{\tilde{\chi}_A^0}^2, m_{\tilde{e}_X}^2 \right) \Big] \\
&+ \Big\{ N_{jBX}^{\mathrm{L}(e)} E_{BA}^{\mathrm{L}(\tilde{\chi}^0)} N_{iAX}^{\mathrm{R}(e)*} \left[m_{\tilde{\chi}_B^0} m_{\tilde{\chi}_A^0} F_1 \left(m_{\tilde{e}_X}^2, m_{\tilde{\chi}_A^0}^2, m_{\tilde{\chi}_B^0}^2 \right) \right] \\
&+ N_{jBX}^{\mathrm{R}(e)} E_{BA}^{\mathrm{L}(\tilde{\chi}^0)} N_{iAX}^{\mathrm{L}(e)*} \left[-2 F_2 (m_{\tilde{e}_X}^2, m_{\tilde{\chi}_A^0}^2, m_{\tilde{\chi}_B^0}^2) \right] \Big\},
\end{aligned} \tag{23}$$

$$\mathcal{P}_Z^{(C)\mathrm{R}} = \mathcal{P}_Z^{(C)\mathrm{L}}(\mathrm{L} \leftrightarrow \mathrm{R}) \,, \tag{24}$$

$$\mathcal{P}_Z^{(N)\mathrm{R}} = \mathcal{P}_Z^{(N)\mathrm{L}}(\mathrm{L} \leftrightarrow \mathrm{R}) \,, \quad E_{BA}^{\mathrm{R}(\tilde{\chi}^0)} = -E_{BA}^{\mathrm{L}(\tilde{\chi}^0)} \,. \tag{25}$$

$E_{BA}^{\mathrm{R}(\tilde{\chi}^-)}$ and $E_{BA}^{\mathrm{L,R}(\tilde{\chi}^0)}$ are constants in the Z-boson–chargino and Z-boson–neutralino vertices, and $D_{YX}^{(\tilde{e})}$ is a constant in the Z-boson–selectron vertex. These constants are defined in Appendix C. G_{Ze}^L and G_{Ze}^R are constants appearing in the SM Ze_ie_j vertices,

$$\begin{aligned}
\mathcal{L}_{Ze_ie_j} = &- g \gamma_\mu \delta_{ij} \{ G_{Ze}^\mathrm{L} P_\mathrm{L} + G_{Ze}^\mathrm{R} P_\mathrm{R} \} \\
&- g \gamma_\mu \delta_{ij} \left\{ \left[-\frac{1}{2} \frac{1}{c_\mathrm{W}} + \frac{s_\mathrm{W}^2}{c_\mathrm{W}} \right] P_\mathrm{L} + \left[\frac{s_\mathrm{W}^2}{c_\mathrm{W}} \right] P_\mathrm{R} \right\},
\end{aligned} \tag{26}$$

$F_1(a,b,c)$ and $F_2(a,b,c)$ are loop functions contained in the triangle-diagram part of the amplitude, and f_1 and f_2 are the loop functions coming from the self-energy part of the amplitude. They are given in Appendix D.

The terms in (22) and (23), which have a corresponding contribution in the photon amplitude (the leading-order photon-penguin amplitude comes from six Feynman diagrams, while the Z-boson-penguin amplitude has eight Feynman diagram contributions), have been compared by replacing Z-boson vertices with the corresponding photon vertices, and agreement has been found. The remaining two Feynman diagram contributions, which are embraced by curly brackets in (22) and (23), have been carefully checked. The new terms in $\mathcal{P}_Z^{(C)\mathrm{L}}$ in comparison with [70] are the third (self-energy-type term) and the fourth term. Further, neither of our terms in $\mathcal{P}_Z^{(C)\mathrm{R}}$ does agree with the amplitude in [70], although the expression in the curly brackets is almost equal to it (in [70] in formula (27), the $\ln x_{AX}$ term should not appear, and in (28) $1/m_{\tilde{\ell}_X}^2$ should be replaced by $1/m_{\tilde{\nu}_X}^2$).

2.2.3 The box form factors

The box contribution to the SL LFV $\ell \to \ell_i \bar{q}_a q_b$ amplitude comes from two box-diagrams in the leading order of perturbation theory. The box amplitude reads

$$\begin{aligned}
\mathcal{M}_\mathrm{box} = \frac{\mathrm{i}}{(4\pi)^2} \sum_{\bar{q}_a q_b = \bar{u}u, \bar{d}d, \bar{s}s, \bar{d}s, \bar{s}d} & \Big[\mathcal{B}_{1\bar{q}_a q_b}^\mathrm{L} (\bar{u}_{\ell_j} \gamma^\mu P_\mathrm{L} u_{\ell_i}) (\bar{u}_{q_a} \gamma_\mu P_\mathrm{L} v_{q_b}) \\
&+ \mathcal{B}_{1\bar{q}_a q_b}^\mathrm{R} (\bar{u}_{\ell_j} \gamma^\mu P_\mathrm{R} u_{\ell_i}) (\bar{u}_{q_a} \gamma_\mu P_\mathrm{R} v_{q_b}) \\
&+ \mathcal{B}_{2\bar{q}_a q_b}^\mathrm{L} (\bar{u}_{\ell_j} \gamma^\mu P_\mathrm{L} u_{\ell_i}) (\bar{u}_{q_a} \gamma_\mu P_\mathrm{R} v_{q_b}) \\
&+ \mathcal{B}_{2\bar{q}_a q_b}^\mathrm{R} (\bar{u}_{\ell_j} \gamma^\mu P_\mathrm{R} u_{\ell_i}) (\bar{u}_{q_a} \gamma_\mu P_\mathrm{L} v_{q_b}) \\
&+ \mathcal{B}_{3\bar{q}_a q_b}^\mathrm{L} (\bar{u}_{\ell_j} P_\mathrm{L} u_{\ell_i}) (\bar{u}_{q_a} P_\mathrm{L} v_{q_b}) \\
&+ \mathcal{B}_{3\bar{q}_a q_b}^\mathrm{R} (\bar{u}_{\ell_j} P_\mathrm{R} u_{\ell_i}) (\bar{u}_{q_a} P_\mathrm{R} v_{q_b}) \\
&+ \bar{\mathcal{B}}_{3\bar{q}_a q_b}^\mathrm{L} (\bar{u}_{\ell_j} P_\mathrm{L} u_{\ell_i}) (\bar{u}_{q_a} P_\mathrm{R} v_{q_b}) \\
&+ \bar{\mathcal{B}}_{3\bar{q}_a q_b}^\mathrm{R} (\bar{u}_{\ell_j} P_\mathrm{R} u_{\ell_i}) (\bar{u}_{q_a} P_\mathrm{L} v_{q_b}) \\
&+ \mathcal{B}_{4\bar{q}_a q_b}^\mathrm{L} (\bar{u}_{\ell_j} \sigma_{\mu\nu} P_\mathrm{L} u_{\ell_i}) (\bar{u}_{q_a} \sigma^{\mu\nu} P_\mathrm{L} v_{q_b}) \\
&+ \mathcal{B}_{4\bar{q}_a q_b}^\mathrm{R} (\bar{u}_{\ell_j} \sigma_{\mu\nu} P_\mathrm{R} u_{\ell_i}) (\bar{u}_{q_a} \sigma^{\mu\nu} P_\mathrm{R} v_{q_b}) \Big].
\end{aligned} \tag{27}$$

The very rich structure of the box-diagram amplitude is a consequence of the Fierz transformation of the terms containing a product of lepton–quark and quark–lepton vector and axial-vector currents. All currents permitted by the Dirac algebra do appear. (The $\ell \to \ell' \ell_1 \ell_2$ box amplitudes studied in [70] do not have so rich a structure – they do not contain $\bar{\mathcal{B}}_{3\bar{q}_a q_b}^{\mathrm{L,R}}$ contributions.) Each box-amplitude form factor has a chargino (C) and a neutralino (N) contribution. We have

$$\mathcal{B}_{i\bar{q}_a q_b}^{\mathrm{L,R}} = \mathcal{B}_{i\bar{q}_a q_b}^{(N)\mathrm{L,R}} + \mathcal{B}_{i\bar{q}_a q_b}^{(C)\mathrm{L,R}} \,, \tag{28}$$

$$\bar{\mathcal{B}}_{3\bar{q}_a q_b}^{\mathrm{L,R}} = \bar{\mathcal{B}}_{3\bar{q}_a q_b}^{(N)\mathrm{L,R}} + \bar{\mathcal{B}}_{3\bar{q}_a q_b}^{(C)\mathrm{L,R}} \,. \tag{29}$$

Here and in the following equations, the indices $\bar{q}_a q_b$ assume the values appearing in the sum in (27). The neutralino contributions read

$$\begin{aligned}\mathcal{B}^{(N)\mathrm{L}}_{1\bar{q}_a q_b} &= \frac{1}{4} d_2\left(M^2_{\tilde{\chi}^0_A}, M^2_{\tilde{\chi}^0_B}, m^2_{\tilde{e}_X}, m^2_{\tilde{q}_Y}\right) \\ &\times N^{\mathrm{R}(e)*}_{iAX} N^{\mathrm{R}(e)}_{jBX} N^{\mathrm{R}(q)*}_{bBY} N^{\mathrm{R}(q)}_{aAY} \\ &+ \frac{1}{2} d_0\left(M^2_{\tilde{\chi}^0_A}, M^2_{\tilde{\chi}^0_B}, m^2_{\tilde{e}_X}, m^2_{\tilde{q}_Y}\right) M_{\tilde{\chi}^0_A} M_{\tilde{\chi}^0_B} \\ &\times N^{\mathrm{R}(e)*}_{iAX} N^{\mathrm{R}(e)*}_{jBX} N^{\mathrm{R}(q)}_{bAY} N^{\mathrm{R}(q)}_{aBY}, \end{aligned} \tag{30}$$

$$\begin{aligned}\mathcal{B}^{(N)\mathrm{L}}_{2\bar{q}_a q_b} &= -\frac{1}{4} d_2\left(M^2_{\tilde{\chi}^0_A}, M^2_{\tilde{\chi}^0_B}, m^2_{\tilde{e}_X}, m^2_{\tilde{q}_Y}\right) \\ &\times N^{\mathrm{R}(e)*}_{iAX} N^{\mathrm{R}(e)}_{jBX} N^{\mathrm{L}(q)*}_{bAY} N^{\mathrm{L}(q)}_{aBY} \\ &- \frac{1}{2} d_0\left(M^2_{\tilde{\chi}^0_A}, M^2_{\tilde{\chi}^0_B}, m^2_{\tilde{e}_X}, m^2_{\tilde{q}_Y}\right) M_{\tilde{\chi}^0_A} M_{\tilde{\chi}^0_B} \\ &\times N^{\mathrm{R}(e)*}_{iAX} N^{\mathrm{R}(e)}_{jBX} N^{\mathrm{L}(q)*}_{bAY} N^{\mathrm{L}(q)}_{aBY}, \end{aligned} \tag{31}$$

$$\begin{aligned}\mathcal{B}^{(N)\mathrm{L}}_{3\bar{q}_a q_b} &= d_0\left(M^2_{\tilde{\chi}^0_A}, M^2_{\tilde{\chi}^0_B}, m^2_{\tilde{e}_X}, m^2_{\tilde{q}_Y}\right) \\ &\times M_{\tilde{\chi}^0_A} M_{\tilde{\chi}^0_B} \Big\{ -\frac{1}{2} N^{\mathrm{R}(e)*}_{iAX} N^{\mathrm{L}(e)}_{jBX} N^{\mathrm{R}(q)*}_{bBY} N^{\mathrm{L}(q)}_{aAY} \\ &- \frac{1}{2} N^{\mathrm{R}(e)*}_{iAX} N^{\mathrm{L}(e)}_{jBX} N^{\mathrm{R}(q)*}_{bAY} N^{\mathrm{L}(q)}_{aBY} \Big\}, \end{aligned} \tag{32}$$

$$\begin{aligned}\bar{\mathcal{B}}^{(N)\mathrm{L}}_{3\bar{q}_a q_b} &= d_2\left(M^2_{\tilde{\chi}^0_A}, M^2_{\tilde{\chi}^0_B}, m^2_{\tilde{e}_X}, m^2_{\tilde{q}_Y}\right) \\ &\times \Big\{ -\frac{1}{2} N^{\mathrm{R}(e)*}_{iAX} N^{\mathrm{L}(e)}_{jBX} N^{\mathrm{L}(q)*}_{bBY} N^{\mathrm{R}(q)}_{aAY} \\ &- \frac{1}{2} N^{\mathrm{R}(e)*}_{iAX} N^{\mathrm{L}(e)}_{jBX} N^{\mathrm{L}(q)*}_{bAY} N^{\mathrm{R}(q)}_{aBY} \Big\}, \end{aligned} \tag{33}$$

$$\begin{aligned}\mathcal{B}^{(N)\mathrm{L}}_{4\bar{q}_a q_b} &= \frac{1}{8} d_0\left(M^2_{\tilde{\chi}^0_A}, M^2_{\tilde{\chi}^0_B}, m^2_{\tilde{e}_X}, m^2_{\tilde{q}_Y}\right) \\ &\times M_{\tilde{\chi}^0_A} M_{\tilde{\chi}^0_B} \Big\{ N^{\mathrm{R}(e)*}_{iAX} N^{\mathrm{L}(e)}_{jBX} N^{\mathrm{R}(q)*}_{bBY} N^{\mathrm{L}(q)}_{aAY} \\ &- N^{\mathrm{R}(e)*}_{iAX} N^{\mathrm{L}(e)}_{jBX} N^{\mathrm{R}(q)*}_{bAY} N^{\mathrm{L}(q)}_{aBY} \Big\}, \end{aligned} \tag{34}$$

$$\mathcal{B}^{(N)\mathrm{R}}_{i\bar{q}_a q_b} = \mathcal{B}^{(N)\mathrm{L}}_{i\bar{q}_a q_b}|_{\mathrm{L}\leftrightarrow\mathrm{R}} \quad (i = 1, \ldots, 4) \tag{35}$$

$$\bar{\mathcal{B}}^{(N)\mathrm{R}}_{3\bar{q}_a q_b} = \bar{\mathcal{B}}^{(N)\mathrm{L}}_{3\bar{q}_a q_b}|_{\mathrm{L}\leftrightarrow\mathrm{R}}\,. \tag{36}$$

The chargino contributions are

$$\begin{aligned}\mathcal{B}^{(C)\mathrm{L}}_{1\bar{q}_a q_b} &= \frac{1}{4} d_2\left(M^2_{\tilde{\chi}^-_A}, M^2_{\tilde{\chi}^-_B}, m^2_{\tilde{\nu}_X}, m^2_{\tilde{q'}_Y}\right) \\ &\times C^{\mathrm{R}(e)*}_{iAX} C^{\mathrm{R}(e)}_{jBX} C^{\mathrm{R}(q)*}_{bBY} C^{\mathrm{R}(q)}_{aAY} \delta_{qd} \\ &+ \frac{1}{2} d_0\left(M^2_{\tilde{\chi}^-_A}, M^2_{\tilde{\chi}^-_B}, m^2_{\tilde{\nu}_X}, m^2_{\tilde{q'}_Y}\right) \\ &\times M_{\tilde{\chi}^-_A} M_{\tilde{\chi}^-_B} C^{\mathrm{R}(e)*}_{iAX} C^{\mathrm{R}(e)*}_{jBX} C^{\mathrm{R}(q)}_{bAY} C^{\mathrm{R}(q)}_{aBY}\, \delta_{qu}, \end{aligned} \tag{37}$$

$$\begin{aligned}\mathcal{B}^{(C)\mathrm{L}}_{2\bar{q}_a q_b} &= -\frac{1}{4} d_2\left(M^2_{\tilde{\chi}^-_A}, M^2_{\tilde{\chi}^-_B}, m^2_{\tilde{\nu}_X}, m^2_{\tilde{q'}_Y}\right) \\ &\times C^{\mathrm{R}(e)*}_{iAX} C^{\mathrm{R}(e)}_{jBX} C^{\mathrm{L}(q)*}_{bAY} C^{\mathrm{L}(q)}_{aBY}\, \delta_{qd} \\ &- \frac{1}{2} d_0\left(M^2_{\tilde{\chi}^-_A}, M^2_{\tilde{\chi}^-_B}, m^2_{\tilde{\nu}_X}, m^2_{\tilde{q'}_Y}\right) \\ &\times M_{\tilde{\chi}^-_A} M_{\tilde{\chi}^-_B} C^{\mathrm{R}(e)*}_{iAX} C^{\mathrm{R}(e)}_{jBX} C^{\mathrm{L}(q)*}_{bAY} C^{\mathrm{L}(q)}_{aBY} \delta_{qu}, \end{aligned} \tag{38}$$

$$\begin{aligned}\mathcal{B}^{(C)\mathrm{L}}_{3\bar{q}_a q_b} &= d_0\left(M^2_{\tilde{\chi}^-_A}, M^2_{\tilde{\chi}^-_B}, m^2_{\tilde{\nu}_X}, m^2_{\tilde{q'}_Y}\right) \\ &\times M_{\tilde{\chi}^-_A} M_{\tilde{\chi}^-_B} \Big\{ -\frac{1}{2} C^{\mathrm{R}(e)*}_{iAX} C^{\mathrm{L}(e)}_{jBX} C^{\mathrm{R}(q)*}_{bBY} C^{\mathrm{L}(q)}_{aAY} \delta_{qd} \\ &- \frac{1}{2} C^{\mathrm{R}(e)*}_{iAX} C^{\mathrm{L}(e)}_{jBX} C^{\mathrm{R}(q)*}_{bAY} C^{\mathrm{L}(q)}_{aBY} \delta_{qu} \Big\}, \end{aligned} \tag{39}$$

$$\begin{aligned}\bar{\mathcal{B}}^{(C)\mathrm{L}}_{3\bar{q}_a q_b} &= d_2\left(M^2_{\tilde{\chi}^-_A}, M^2_{\tilde{\chi}^-_B}, m^2_{\tilde{\nu}_X}, m^2_{\tilde{q'}_Y}\right) \\ &\times \Big\{ -\frac{1}{2} C^{\mathrm{R}(e)*}_{iAX} C^{\mathrm{L}(e)}_{jBX} C^{\mathrm{L}(q)*}_{bBY} C^{\mathrm{R}(q)}_{aAY} \delta_{qd} \\ &- \frac{1}{2} C^{\mathrm{R}(e)*}_{iAX} C^{\mathrm{L}(e)}_{jBX} C^{\mathrm{L}(q)*}_{bAY} C^{\mathrm{R}(q)}_{aBY} \delta_{qu} \Big\}, \end{aligned} \tag{40}$$

$$\begin{aligned}\mathcal{B}^{(C)\mathrm{L}}_{4\bar{q}_a q_b} &= \frac{1}{8} d_0\left(M^2_{\tilde{\chi}^-_A}, M^2_{\tilde{\chi}^-_B}, m^2_{\tilde{\nu}_X}, m^2_{\tilde{q'}_Y}\right) \\ &\times M_{\tilde{\chi}^-_A} M_{\tilde{\chi}^-_B} \Big\{ C^{\mathrm{R}(e)*}_{iAX} C^{\mathrm{L}(e)}_{jBX} C^{\mathrm{R}(q)*}_{bBY} C^{\mathrm{L}(q)}_{aAY} \delta_{qd} \\ &- C^{\mathrm{R}(e)*}_{iAX} C^{\mathrm{L}(e)}_{jBX} C^{\mathrm{R}(q)*}_{bAY} C^{\mathrm{L}(q)}_{aBY} \delta_{qu} \Big\}, \end{aligned} \tag{41}$$

$$\mathcal{B}^{(C)\mathrm{R}}_{i\bar{q}_a q_b} = \mathcal{B}^{(C)\mathrm{L}}_{i\bar{q}_a q_b}\Big|_{\mathrm{L}\leftrightarrow\mathrm{R}} \quad (i = 1, \ldots, 4)\,, \tag{42}$$

where $q' = d(u)$ for $q = u(d)$. Summing over paired indices is assumed. The Kronecker function δ_{qu} [δ_{qd}] denotes that the q quark is one of the up (u, c or t) quarks [one of the down quarks]. The loop functions d_0 and d_2 are evaluated by neglecting the momenta of incoming and outgoing particles. They are listed in Appendix D.

3 Amplitudes and branching ratios

3.1 Hadronization of currents

The effective Lagrangians (the matrix elements) for photon and Z-boson part of the amplitudes for SL LFV lepton decays comprise vector and axial-vector currents, while the box amplitude contains all possible quark currents permitted by the Dirac algebra, that is scalar-, pseudoscalar-, vector-, axial-vector- and tensor-quark currents. To perform a calculation of the charged-lepton SL LFV decays rates, these currents have to be converted into meson currents comprising the mesons states studied of the final products of the charged-lepton SL LFV decays. The hadronization procedure we use here is not exact in the sense that we do not include the sea-quark and gluon content of the meson fields, but it is precise enough to give much better than an order of magnitude decay rates of the processes considered. The quark content of the meson states is given in Appendix E. The hadronization of the axial-vector current is achieved through PCAC (see e.g. [105–107]; for the normalization of the pseudoscalar coupling constants used here and for further details see [44]). The hadronization of the vector current is achieved using the vector-meson-dominance assumption (see [106, 107]; for the normalization of the vector-meson decay constant and details see [44, 45, 108]). Hadronization of scalar currents is achieved by comparing the quark sector of the SM Lagrangian and the corresponding effective meson Lagrangian [109–111] (for applications in

the context of LFV and details see [45]). Hadronization of the pseudoscalar current is obtained by the same procedure as for the scalar current. The results obtained by using this procedure are equal to the results obtained by using the equation of motion for the current-quark masses (see e.g. [112]) and the results for hadronization of the axial-vector current, up to the difference of the up and down quark masses and/or up to the difference of the pseudoscalar decay constants. The hadronization of the tensor-quark currents is obtained by comparing the derivative of the tensor-quark current with a vector-quark current and using the equations of motion for the current-quark masses. The difference between the terms, one containing the derivative of the incoming quark field and the other containing the derivative of the outgoing quark field, have been neglected. The error expected from this approximation is proportional to the amount of breaking of the $\mathrm{SU}(3)_{\mathrm{flavor}}$ symmetry. The tensor currents are proportional to the current-quark masses, and therefore they give a smaller contribution than the other quark currents. Therefore, the error introduced by this approximation in the total SL LFV amplitude is small.

Here we summarize the basic quantities needed to describe the hadronization of quark currents:

1. the pseudoscalar meson decay constants [113] (f_P, $P = \pi^0, \eta, \eta', K^0, \bar{K}^0$);
2. the constants γ_V [108] ($V = \rho^0, \phi, \omega, K^{*0}, \bar{K}^{*0}$) defining the vector-meson decay constants ($f_V \sim m_V^2/\gamma_V$);
3. the mixing angles θ_P and θ_V [113] defining the physical meson-nonet states in terms of the unphysical singlet and octet meson states;
4. the parameter r [109–111] (m_u, m_d and m_s are the current-quark masses), with

$$r = \frac{2m_{\pi^+}^2}{m_u + m_d} = \frac{2m_{K^0}^2}{m_d + m_s} = \frac{2m_{K^+}^2}{m_u + m_s}\,, \qquad (43)$$

that appears in the hadronization procedure for the scalar and pseudoscalar currents.

Having the identification of the quark currents with the corresponding meson currents, achieved by the above hadronization procedure, one can write down the effective Lagrangian as a sum of terms with an incoming lepton field ℓ_i and an outgoing lepton field ℓ_j and pseudoscalar-meson (P) or vector-meson (V) field(s). This Lagrangian directly gives the amplitudes for the $\ell_i \to \ell_j P(V)$ processes. Amplitudes with a pseudoscalar meson in the final state contributions come from the pseudoscalar and axial-vector coupling part of the effective Lagrangian, while the amplitudes with a vector meson have vector and tensor coupling contributions. Only the scalar coupling gives no contribution to the one-meson processes in the final state, $\ell_i \to \ell_j P(V)$. It contributes only to the processes with two pseudoscalar mesons in the final state, $\ell_i \to \ell_j P_1 P_2$.

3.2 Vector-meson–pseudoscalar-meson interactions

The processes with two pseudoscalar mesons in the final state are generated by the scalar-quark-current part of the effective Lagrangian and the vector-quark- and tensor-quark current of the effective Lagrangian. The scalar-quark-current part of the effective Lagrangian produces two pseudoscalar fields directly. The vector-quark- and tensor-quark-current parts produce a resonant vector-meson state (V), which decays into two pseudoscalar mesons (P). The VPP interactions necessary for the description of the VPP interactions appearing in the charged-lepton SL LFV decays are described by the part of the meson Lagrangian containing these VPP vertices [45]

$$\begin{aligned}
&\mathcal{L}_{VPP} = \\
&\quad -\frac{\mathrm{i}g_{\rho\pi\pi}}{2}\Big\{\rho^{0,\mu}\left(2\pi^+\overset{\leftrightarrow}{\partial}_\mu\pi^- + K^+\overset{\leftrightarrow}{\partial}_\mu K^- - K^0\overset{\leftrightarrow}{\partial}_\mu\bar{K}^0\right)\\
&\quad +\sqrt{3}s_V\omega^\mu\left(K^+\overset{\leftrightarrow}{\partial}_\mu K^- + K^0\overset{\leftrightarrow}{\partial}_\mu\bar{K}^0\right)\\
&\quad +\sqrt{3}c_V\phi^\mu\left(K^+\overset{\leftrightarrow}{\partial}_\mu K^- + K^0\overset{\leftrightarrow}{\partial}_\mu\bar{K}^0\right)\\
&\quad +K^{0*,\mu}\Big(-\sqrt{2}\pi^+\overset{\leftrightarrow}{\partial}_\mu K^- + \pi^0\overset{\leftrightarrow}{\partial}_\mu\bar{K}^0\\
&\quad +\sqrt{3}c_P\bar{K}^0\overset{\leftrightarrow}{\partial}_\mu\eta + \sqrt{3}s_P\bar{K}^0\overset{\leftrightarrow}{\partial}_\mu\eta'\Big)\\
&\quad +\bar{K}^{0*,\mu}\Big(\sqrt{2}\pi^-\overset{\leftrightarrow}{\partial}_\mu K^+ - \pi^0\overset{\leftrightarrow}{\partial}_\mu K^0 - \sqrt{3}c_P K^0\overset{\leftrightarrow}{\partial}_\mu\eta\\
&\quad -\sqrt{3}s_P K^0\overset{\leftrightarrow}{\partial}_\mu\eta'\Big)\Big\} + \ldots \qquad (44)
\end{aligned}$$

This Lagrangian is a part of the nonlinear $(\mathrm{U}(3)_\mathrm{L} \times \mathrm{U}(3)_\mathrm{R})/\mathrm{U}(3)_V$ symmetric sigma-model Lagrangian. The $\mathrm{U}(3)_V$ symmetry corresponds to the vector mesons in the linear realization of the gauge equivalent $(\mathrm{U}(3)_\mathrm{L} \times \mathrm{U}(3)_\mathrm{R})_{\mathrm{global}} \times \mathrm{U}(3)_V$ linear sigma-model [114, 115]. One can include the $(\mathrm{U}(3)_\mathrm{L} \times \mathrm{U}(3)_\mathrm{R})/\mathrm{U}(3)_V$ breaking terms too [115]. That was applied to SL LFV tau-lepton decays in [45], but for the estimates of the charged-lepton SL LFV decays it is an unnecessary complication, and we will not consider it here.

From (44) one can read the $c_{VP_1P_2}$ couplings in terms of the $g_{\rho\pi\pi}$ coupling. For instance, $c_{\rho^0K^+K^-} = \frac{1}{2}g_{\rho\pi\pi}$.

When the amplitudes by vector-meson resonance(s) are formed, the square of the vector-meson mass in the m_V^2/γ_V, appearing in every vector-meson decay constant, has to be replaced with $(m_V^2 - \mathrm{i}m_V\Gamma_V)/\gamma_V$, where Γ_V is the decay width of the vector meson [45].

The intermediate axial-vector-meson and scalar-meson contributions to lepton LFV amplitudes are not included for the following reasons. Axial mesons decay into three pseudoscalar mesons and therefore they do not contribute to the LFV processes with one or two mesons in the final state. Vector-meson dominance is experimentally well established, and therefore the scalar-meson contributions are highly suppressed.

3.3 Charged-lepton SL LFV with one meson in the final state

Now we can write all amplitudes we are interested in. They are

$$
\begin{aligned}
\mathrm{i}\mathcal{M}^{\ell_i\to\ell_j V} = \mathrm{i}\bar{u}_{\ell_j}\Bigg[& \left(\gamma_\mu - \frac{q_\mu \gamma\cdot q}{q^2}\right) P_{\mathrm{L}} \mathcal{P}^{ijV}_{1\gamma L} \\
& + \left(\gamma_\mu - \frac{q_\mu \gamma\cdot q}{q^2}\right) P_{\mathrm{R}} \mathcal{P}^{ijV}_{1\gamma \mathrm{R}} \\
& + \frac{\mathrm{i}\sigma_{\mu\nu} P_{\mathrm{L}} q^\nu}{q^2} \mathcal{P}^{ijV}_{2\gamma L} + \frac{\mathrm{i}\sigma_{\mu\nu} P_{\mathrm{R}} q^\nu}{q^2} \mathcal{P}^{ijV}_{2\gamma R} \\
& + \gamma_\mu P_{\mathrm{L}} \left(\mathcal{P}^{ijV}_{Z\mathrm{L}} + \mathcal{B}^{ijV}_{1\mathrm{L}}\right) + \gamma_\mu P_{\mathrm{R}} \left(\mathcal{P}^{ijV}_{Z\mathrm{R}} + \mathcal{B}^{ijV}_{1\mathrm{R}}\right) \\
& + \mathrm{i}\sigma_{\mu\nu} P_{\mathrm{L}} q^\nu \mathcal{B}^{ijV}_{2L} + \mathrm{i}\sigma_{\mu\nu} P_{\mathrm{R}} q^\nu \mathcal{B}^{ijV}_{2R} \Bigg] u_{\ell_i} \varepsilon^{\mu\dagger}_V \,.
\end{aligned} \tag{45}
$$

$$
\begin{aligned}
\mathrm{i}\mathcal{M}^{\ell_i\to\ell_j P} = \mathrm{i}\bar{u}_{\ell_j}\Bigg\{ & \Big[\gamma_\mu P_{\mathrm{L}} \left(\mathcal{P}^{ijP}_{Z\mathrm{L}} + \mathcal{B}^{ijP}_{1\mathrm{L}}\right) + \gamma_\mu P_{\mathrm{R}} \\
& \times \left(\mathcal{P}^{ijP}_{Z\mathrm{R}} + \mathcal{B}^{ijP}_{1\mathrm{R}}\right)\Big] q^\mu \\
& + \left[P_{\mathrm{L}} \mathcal{B}^{ijP}_{2L} + P_{\mathrm{R}} \mathcal{B}^{ijP}_{2R}\right] \Bigg\} u_{\ell_i}.
\end{aligned} \tag{46}
$$

The form factors in (45) and (46) are defined by

$$
\mathcal{P}^{ijV}_{a\gamma \mathrm{L,R}} = -e^2 \mathcal{P}^{\mathrm{L,R}}_{a\gamma} \frac{m_V}{\sqrt{2}\gamma_V} k^V_\gamma, \quad (a = 1, 2), (V = \rho^0, \phi, \omega)\,, \tag{47}
$$

$$
\mathcal{P}^{ijV}_{Z\mathrm{L,R}} = \frac{g_Z^2}{m_Z^2 c_{\mathrm{W}}^2} \mathcal{P}^{\mathrm{L,R}}_Z \frac{m_V^2}{\sqrt{2}\gamma_V} k^V_Z, \quad (V = \rho^0, \phi, \omega) \tag{48}
$$

$$
\begin{aligned}
\mathcal{B}^{ijV}_{1\mathrm{L,R}} = & \frac{m_V^2}{\sqrt{2}\gamma_V} \frac{1}{2} \Big[k^V_{\bar{u}u} \left(\mathcal{B}^{\mathrm{L,R}}_{1\bar{u}u} + \mathcal{B}^{\mathrm{L,R}}_{2\bar{u}u}\right) + k^V_{\bar{d}d} \left(\mathcal{B}^{\mathrm{L,R}}_{1\bar{d}d} + \mathcal{B}^{\mathrm{L,R}}_{2\bar{d}d}\right) \\
& + k^V_{\bar{s}s} \left(\mathcal{B}^{\mathrm{L,R}}_{1\bar{s}s} + \mathcal{B}^{\mathrm{L,R}}_{2\bar{s}s}\right) + k^V_{\bar{d}s} \left(\mathcal{B}^{\mathrm{L,R}}_{1\bar{d}s} + \mathcal{B}^{\mathrm{L,R}}_{2\bar{d}s}\right) \\
& + k^V_{\bar{s}d} \left(\mathcal{B}^{\mathrm{L,R}}_{1\bar{s}d} + \mathcal{B}^{\mathrm{L,R}}_{2\bar{s}d}\right)\Big] \,, \\
& (V = \rho^0, \phi, \omega, K^{*0}, \overline{K^{*0}})\,,
\end{aligned} \tag{49}
$$

$$
\begin{aligned}
\mathcal{B}^{ijV}_{2\mathrm{L,R}} = & \frac{-2\sqrt{2}}{\gamma_V} \Big[k^V_{\bar{d}s} (m_d - m_s) \mathcal{B}^{\mathrm{L,R}}_{4\bar{d}s} \\
& + k^V_{\bar{s}d} (m_s - m_d) \mathcal{B}^{\mathrm{L,R}}_{4\bar{s}d}\Big] \,, \quad (V = K^{*0}, \overline{K^{*0}})\,,
\end{aligned} \tag{50}
$$

$$
\mathcal{P}^{ijP}_{Z\mathrm{L,R}} = \frac{g^2}{m_Z^2 c_{\mathrm{W}}^2} \mathcal{P}^{\mathrm{L,R}}_Z (-\sqrt{2} f_P) k^P_Z \quad (P = \pi^0, \eta, \eta')\,, \tag{51}
$$

$$
\begin{aligned}
\mathcal{B}^{ijP}_{1\mathrm{L,R}} = & s_{\mathrm{L,R}} (\sqrt{2} f_P) \frac{1}{2} \Big[k^P_{\bar{u}u} \left(-\mathcal{B}^{\mathrm{L,R}}_{1\bar{u}u} + \mathcal{B}^{\mathrm{L,R}}_{2\bar{u}u}\right) \\
& + k^P_{\bar{d}d} \left(-\mathcal{B}^{\mathrm{L,R}}_{1\bar{d}d} + \mathcal{B}^{\mathrm{L,R}}_{2\bar{d}d}\right) + k^P_{\bar{s}s} \left(-\mathcal{B}^{\mathrm{L,R}}_{1\bar{s}s} + \mathcal{B}^{\mathrm{L,R}}_{2\bar{s}s}\right) \\
& + k^P_{\bar{d}s} \left(-\mathcal{B}^{\mathrm{L,R}}_{1\bar{d}s} + \mathcal{B}^{\mathrm{L,R}}_{2\bar{d}s}\right) + k^P_{\bar{s}d} \left(-\mathcal{B}^{\mathrm{L,R}}_{1\bar{s}d} + \mathcal{B}^{\mathrm{L,R}}_{2\bar{s}d}\right)\Big] \,, \\
& (P = \pi^0, \eta, \eta', K^0, \overline{K^0})\,,
\end{aligned} \tag{52}
$$

$$
\begin{aligned}
\mathcal{B}^{ijP}_{2\mathrm{L,R}} = & s_{\mathrm{L,R}} \left(-\frac{ir}{2}\right) (\sqrt{2} f_P) \frac{1}{2} \Big[k^P_{\bar{u}u} \left(-\mathcal{B}^{\mathrm{L,R}}_{3\bar{u}u} + \overline{\mathcal{B}}^{\mathrm{L,R}}_{3\bar{u}u}\right) \\
& + k^P_{\bar{d}d} \left(-\mathcal{B}^{\mathrm{L,R}}_{3\bar{d}d} + \overline{\mathcal{B}}^{\mathrm{L,R}}_{3\bar{d}d}\right) + k^P_{\bar{s}s} \left(-\mathcal{B}^{\mathrm{L,R}}_{3\bar{s}s} + \overline{\mathcal{B}}^{\mathrm{L,R}}_{3\bar{s}s}\right) \\
& + k^P_{\bar{d}s} \left(-\mathcal{B}^{\mathrm{L,R}}_{3\bar{d}s} + \overline{\mathcal{B}}^{\mathrm{L,R}}_{3\bar{d}s}\right) + k^P_{\bar{s}d} \left(-\mathcal{B}^{\mathrm{L,R}}_{3\bar{s}d} + \overline{\mathcal{B}}^{\mathrm{L,R}}_{3\bar{s}d}\right)\Big] \,, \\
& (P = \pi^0, \eta, \eta', K^0, \overline{K^0})\,.
\end{aligned} \tag{53}
$$

In (52) and (53) $s_{\mathrm{L}} = 1$ and $s_{\mathrm{R}} = -1$. The constants k^V_γ, k^V_Z, k^P_Z, and $k^V_{\bar{q}_a q_b}$ are defined in Appendix E.

A branching ratio for the processes $\ell_i \to \ell_j P$ with unpolarized initial and final particles reads

$$
\begin{aligned}
B(\ell_i \to \ell_j P) = & \frac{1}{8\pi} \frac{1}{m_i^2} \frac{1}{\Gamma_{\ell_i}} \frac{\lambda^{\frac{1}{2}}(m_i^2, m_j^2, m_P^2)}{2m_i} \\
& \times \Big[\left(\left|\mathcal{P}^{ijP}_{Z\mathrm{L}} + \mathcal{B}^{ijP}_{1\mathrm{L}}\right|^2 + \left|\mathcal{P}^{ijP}_{Z\mathrm{R}} + \mathcal{B}^{ijP}_{1\mathrm{R}}\right|^2\right) i_{P1} \\
& + \left(\left|\mathcal{B}^{ijP}_{2L}\right|^2 + \left|\mathcal{B}^{ijP}_{2R}\right|^2\right) i_{P2} \\
& + \left(\left(\mathcal{P}^{ijP}_{Z\mathrm{L}} + \mathcal{B}^{ijP}_{1\mathrm{L}}\right)\left(\mathcal{P}^{ijP}_{Z\mathrm{R}} + \mathcal{B}^{ijP}_{1\mathrm{R}}\right)^* + \mathrm{c.c.}\right) \\
& \times m_j m_i i_{P3} + \Big(\left(\mathcal{P}^{ijP}_{Z\mathrm{L}} + \mathcal{B}^{ijP}_{1\mathrm{L}}\right)\left(\mathcal{B}^{ijP}_{2L}\right)^* \\
& + \left(\mathcal{P}^{ijP}_{Z\mathrm{R}} + \mathcal{B}^{ijP}_{1\mathrm{R}}\right)\left(\mathcal{B}^{ijP}_{2R}\right)^* + \mathrm{c.c.}\Big) m_j i_{P4} \\
& + \Big(\left(\mathcal{P}^{ijP}_{Z\mathrm{L}} + \mathcal{B}^{ijP}_{1\mathrm{L}}\right)\left(\mathcal{B}^{ijP}_{2R}\right)^* \\
& + \left(\mathcal{P}^{ijP}_{Z\mathrm{R}} + \mathcal{B}^{ijP}_{1\mathrm{R}}\right)\left(\mathcal{B}^{ijP}_{2L}\right)^* + \mathrm{c.c.}\Big) m_i i_{P5} \\
& + \left((\mathcal{B}^{ijP}_{2L})(\mathcal{B}^{ijP}_{2R})^* + \mathrm{c.c.}\right) m_i m_j\Big] \,,
\end{aligned} \tag{54}
$$

where Γ_{ℓ_i} is the total decay rate of the lepton ℓ_i,

$$
\begin{aligned}
i_{P1} &= \frac{1}{2}\left((m_i^2 - m_j^2)^2 - (m_i^2 + m_j^2) m_P^2\right) \,, \\
i_{P2} &= \frac{1}{2}(m_i^2 + m_j^2 - m_P^2)\,, \\
i_{P3} &= m_P^2\,, \\
i_{P4} &= \frac{1}{2}(m_i^2 + m_P^2 - m_j^2)\,, \\
i_{P5} &= \frac{1}{2}(m_i^2 - m_P^2 - m_j^2)\,,
\end{aligned} \tag{55}
$$

and

$$
\lambda(x, y, z) = x^2 + y^2 + z^2 - 2xy - 2xz - 2yz\,. \tag{56}
$$

The branching ratio for the processes $\ell_i \to \ell_j V$ with unpolarized initial and final particles reads

$$
\begin{aligned}
B(\ell_i \to \ell_j V) = & \frac{1}{8\pi} \frac{1}{\Gamma_{\ell_i}} \frac{1}{m_i^2} \frac{\lambda^{\frac{1}{2}}(m_i^2, m_j^2, m_V^2)}{2m_i} \\
& \times \Big[\left(\left|\mathcal{P}^{ijV}_{1\gamma L} + \mathcal{P}^{ijV}_{Z\mathrm{L}} + \mathcal{B}^{ijV}_{1\mathrm{L}}\right|^2 + \left|\mathcal{P}^{ijV}_{1\gamma \mathrm{R}} + \mathcal{P}^{ijV}_{Z\mathrm{R}} + \mathcal{B}^{ijV}_{1\mathrm{R}}\right|^2\right) i_{V1} \\
& + \left(\left|\frac{\mathcal{P}^{ijV}_{2\gamma L}}{m_V^2} + \mathcal{B}^{ijV}_{2L}\right|^2 + \left|\frac{\mathcal{P}^{ijV}_{2\gamma R}}{m_V^2} + \mathcal{B}^{ijV}_{2R}\right|^2\right) i_{V2} \\
& + \left(\left(\mathcal{P}^{ijV}_{1\gamma \mathrm{L}} + \mathcal{P}^{ijV}_{Z\mathrm{L}} + \mathcal{B}^{ijV}_{1\mathrm{L}}\right)\left(\mathcal{P}^{ijV}_{1\gamma \mathrm{R}} + \mathcal{P}^{ijV}_{Z\mathrm{R}} + \mathcal{B}^{ijV}_{1\mathrm{R}}\right)^* + \mathrm{c.c.}\right) \\
& \times (-m_i m_j) + \left(\left(\frac{\mathcal{P}^{ijV}_{2\gamma L}}{m_V^2} + \mathcal{B}^{ijV}_{2L}\right)\left(\frac{\mathcal{P}^{ijV}_{2\gamma R}}{m_V^2} + \mathcal{B}^{ijV}_{2R}\right)^* + \mathrm{c.c.}\right) \\
& \times (-m_V^2 m_i m_j) + \left((\mathcal{P}^{ijV}_{1\gamma L} + \mathcal{P}^{ijV}_{Z\mathrm{L}} + \mathcal{B}^{ijV}_{1\mathrm{L}})\left(\frac{\mathcal{P}^{ijV}_{2\gamma L}}{m_V^2} + \mathcal{B}^{ijV}_{2L}\right)^*\right. \\
& \left. + \left(\mathcal{P}^{ijV}_{1\gamma \mathrm{R}} + \mathcal{P}^{ijV}_{Z\mathrm{R}} + \mathcal{B}^{ijV}_{1\mathrm{R}}\right)\left(\frac{\mathcal{P}^{ijV}_{2\gamma R}}{m_V^2} + \mathcal{B}^{ijV}_{2R}\right)^* + \mathrm{c.c.}\right)(m_j i_{V3})
\end{aligned}
$$

$$+\left(\left(\mathcal{P}^{ijV}_{1\gamma L}+\mathcal{P}^{ijV}_{ZL}+\mathcal{B}^{ijV}_{1L}\right)\left(\frac{\mathcal{P}^{ijV}_{2\gamma R}}{m_V^2}+\mathcal{B}^{ijV}_{2R}\right)^*\right.$$
$$\left.+(\mathcal{P}^{ijV}_{1\gamma R}+\mathcal{P}^{ijV}_{ZR}+\mathcal{B}^{ijV}_{1R})\left(\frac{\mathcal{P}^{ijV}_{2\gamma L}}{m_V^2}+\mathcal{B}^{ijV}_{2L}\right)^*+\text{c.c.}\right)$$
$$\left.\times(m_i i_{V4})\right], \tag{57}$$

where

$$i_{V1}=\frac{1}{2m_V^2}\left[m_V^2(m_i^2+m_j^2)+(m_i^2-m_j^2)^2-2m_V^4\right],$$
$$i_{V2}=(m_i^2-m_j^2)^2-\frac{1}{2}m_V^2(m_i^2+m_j^2)-\frac{1}{2}m_V^4,$$
$$i_{V3}=\frac{1}{2}\left(m_i^2-m_j^2+m_V^2\right),$$
$$i_{V4}=\frac{1}{2}\left(m_i^2-m_j^2-m_V^2\right). \tag{58}$$

3.4 SL LFV decays of a lepton with two pseudoscalar mesons in the final state

The amplitude for the general $\ell_i\to\ell_j P_1P_2$ decay rate is a sum of a scalar-current contribution and resonance contributions (coming from vector- and tensor-current contributions)

$$\mathrm{i}\mathcal{M}^{\ell_i\to\ell_j P_1P_2}=\mathrm{i}\mathcal{M}^{\ell_i\to\ell_j P_1P_2}_{\text{res}}+\mathrm{i}\mathcal{M}^{\ell_i\to\ell_j P_1P_2}_{1}, \tag{59}$$

where

$$\mathcal{M}^{\ell_i\to\ell_j P_1P_2}_{\text{res}}=\mathrm{i}\bar{u}_{\ell_j}\left[D^{P_1P_2}_{1L}\left((\not{p}_2-\not{p}_1)-\frac{m_2^2-m_1^2}{q^2}\not{q}\right)P_L\right.$$
$$+D^{P_1P_2}_{1R}\left((\not{p}_2-\not{p}_1)-\frac{m_2^2-m_1^2}{q^2}\not{q}\right)P_R$$
$$+E^{P_1P_2}_{1L}\mathrm{i}\sigma_{\mu\nu}P_L(p_1-p_2)^\mu q^\nu$$
$$\left.+E^{P_1P_2}_{1R}\mathrm{i}\sigma_{\mu\nu}P_R(p_1-p_2)^\mu q^\nu\right]u_{\ell_i}, \tag{60}$$
$$\mathrm{i}\mathcal{M}^{\ell_i\to\ell_j P_1P_2}_{1}=\mathrm{i}\bar{u}_{\ell_j}\left[P_L A^L_{1P_1P_2}+P_R A^R_{1P_1P_2}\right]u_{\ell_i}. \tag{61}$$

In (61) $D^{P_1P_2}_{1L,R}$ and $E^{P_1P_2}_{1L,R}$ are form factors built from the trilinear $c_{VP_1P_2}$ couplings (defined by the Lagrangian (44)), normalized vector-meson propagators,

$$\frac{m_V^2-\mathrm{i}m_V\Gamma_V}{q^2-m_V^2+\mathrm{i}m_V\Gamma_V} \tag{62}$$

and form factors for $\ell_i\to\ell_j V$ processes divided by the mass of the resonant vector meson, e.g.

$$\tilde{\mathcal{P}}^{ijV}_{1\gamma L,R}=\frac{\mathcal{P}^{ijV}_{1\gamma L,R}}{m_V^2}. \tag{63}$$

The expressions for the $D^{P_1P_2}_{1L,R}$ and $E^{P_1P_2}_{1L,R}$ form factors are

$$D^{P_1P_2}_{1L,R}=\sum_V\left(\tilde{\mathcal{P}}^{ijV}_{1\gamma L,R}+\tilde{\mathcal{P}}^{ijV}_{ZL,R}+\tilde{\mathcal{B}}^{ijV}_{1L,R}\right)$$
$$\times\frac{m_V^2-\mathrm{i}m_V\Gamma_V}{q^2-m_V^2+\mathrm{i}m_V\Gamma_V}c_{VP_1P_2}, \tag{64}$$
$$E^{P_1P_2}_{1L,R}=\sum_V\left(\frac{\tilde{\mathcal{P}}^{ijV}_{2\gamma L,R}}{q^2}+\tilde{\mathcal{B}}^{ijV}_{2L,R}\right)$$
$$\times\frac{m_V^2-\mathrm{i}m_V\Gamma_V}{q^2-m_V^2+\mathrm{i}m_V\Gamma_V}c_{VP_1P_2}. \tag{65}$$

The sum goes over neutral vector mesons only ($V=\rho^0,\phi,\omega,K^{*0},\overline{K^{*0}}$). The coefficients of the non-resonant part of the amplitude, $A_{1P_1P_2}$, are defined as the coefficients of the P_1P_2 product of fields contained in the matrix-valued operator

$$\frac{r}{4}\sum_{q_a,q_b=u,d,s}(\Pi^2)_{\bar{q}_b q_a}\left(\mathcal{B}^{L,R}_{3\bar{q}_a q_b}+\overline{\mathcal{B}}^{L,R}_{3\bar{q}_a q_b}\right), \tag{66}$$

where Π is the matrix of the pseudoscalar fields

$$\Pi=\begin{pmatrix}\pi^0+\frac{1}{\sqrt{3}}\eta_8+\frac{\sqrt{2}}{\sqrt{3}}\eta_1 & \sqrt{2}\pi^+ & \sqrt{2}K^+\\ \sqrt{2}\pi^- & -\pi^0+\frac{1}{\sqrt{3}}\eta_8+\frac{\sqrt{2}}{\sqrt{3}}\eta_1 & \sqrt{2}K^0\\ \sqrt{2}K^- & \sqrt{2}\bar{K}^0 & -\frac{2}{\sqrt{3}}\eta_8+\frac{\sqrt{2}}{\sqrt{3}}\eta_1\end{pmatrix}. \tag{67}$$

For example,

$$A^{L,R}_{1\pi^0\pi^0}=\frac{r}{4}\left[\frac{1}{2}\left(\mathcal{B}^{L,R}_{3\bar{u}u}+\overline{\mathcal{B}}^{L,R}_{3\bar{u}u}+\mathcal{B}^{L,R}_{3\bar{d}d}+\overline{\mathcal{B}}^{L,R}_{3\bar{d}d}\right)\right]. \tag{68}$$

Having the amplitudes, one can easily evaluate the branching fractions. We assume that incoming and outgoing particles are not polarised. We have

$$B(\ell_i\to\ell_j P_1P_2)=\frac{1}{(2\pi)^2}\frac{1}{\Gamma_{\ell_i}}\frac{1}{32m_i^3}\int_{(m_1+m_2)^2}^{(m_i-m_j)^2}\mathrm{d}s_{12}$$
$$\times\int_{s_{j2}^{\min}}^{s_{j2}^{\max}}\mathrm{d}s_{j2}|\mathcal{M}^{\ell_i\to\ell_j P_1P_2}|^2$$
$$=\frac{1}{(2\pi)^2}\frac{1}{32m_i^3}\int_{(m_1+m_2)^2}^{(m_i-m_j)^2}\mathrm{d}s_{12}$$
$$\times\left[\left(\left|D^{P_1P_2}_{1L}\right|^2+\left|D^{P_1P_2}_{1R}\right|^2\right)\bar{I}_1\right.$$
$$+\left(\left|E^{P_1P_2}_{1L}\right|^2+\left|E^{P_1P_2}_{1R}\right|^2\right)\bar{I}_2$$
$$+\left(\left|A^L_{1P_1P_2}\right|^2+\left|A^R_{1P_1P_2}\right|^2\right)\bar{I}_3$$
$$\left.+\left(\left(D^{P_1P_2}_{1L}\right)\left(D^{P_1P_2}_{1R}\right)^*+\text{c.c.}\right)\bar{I}_4\right.$$

$$
\begin{aligned}
&+\left(\left(E_{1\mathrm{L}}^{P_1P_2}\right)\left(E_{1\mathrm{R}}^{P_1P_2}\right)^{*}+\mathrm{c.c.}\right)\bar{I}_5\\
&+\left(\left(A_{1P_1P_2}^{\mathrm{L}}\right)\left(A_{1P_1P_2}^{\mathrm{R}}\right)^{*}+\mathrm{c.c.}\right)\bar{I}_6\\
&+\left(\left(D_{1\mathrm{L}}^{P_1P_2}\right)\left(E_{1\mathrm{L}}^{P_1P_2}\right)^{*}+\left(D_{1\mathrm{R}}^{P_1P_2}\right)\left(E_{1\mathrm{R}}^{P_1P_2}\right)^{*}+\mathrm{c.c.}\right)\bar{I}_7\\
&+\left(\left(D_{1\mathrm{L}}^{P_1P_2}\right)\left(E_{1\mathrm{R}}^{P_1P_2}\right)^{*}+\left(D_{1\mathrm{R}}^{P_1P_2}\right)\left(E_{1\mathrm{L}}^{P_1P_2}\right)^{*}+\mathrm{c.c.}\right)\bar{I}_8\\
&+\left(\left(D_{1\mathrm{L}}^{P_1P_2}\right)\left(A_{1P_1P_2}^{\mathrm{L}}\right)^{*}+\left(D_{1\mathrm{R}}^{P_1P_2}\right)\left(A_{1P_1P_2}^{\mathrm{R}}\right)^{*}+\mathrm{c.c.}\right)\bar{I}_9\\
&+\left(\left(D_{1\mathrm{L}}^{P_1P_2}\right)\left(A_{1P_1P_2}^{\mathrm{R}}\right)^{*}+\left(D_{1\mathrm{R}}^{P_1P_2}\right)\left(A_{1P_1P_2}^{\mathrm{L}}\right)^{*}+\mathrm{c.c.}\right)\bar{I}_{10}\\
&+\left(\left(E_{1\mathrm{L}}^{P_1P_2}\right)\left(A_{1P_1P_2}^{\mathrm{L}}\right)^{*}+\left(E_{1\mathrm{R}}^{P_1P_2}\right)\left(A_{1P_1P_2}^{\mathrm{R}}\right)^{*}+\mathrm{c.c.}\right)\bar{I}_{11}\Bigg].
\end{aligned}
\tag{69}
$$

The Mandelstam variables are defined as $s_{ab}=(p_a-p_b)^2$, e.g. $s_{12}=(p_1-p_2)^2$. The kinematical bounds on the Mandelstam variables $s_{j2}^{\min}$ and $s_{j2}^{\max}$ are well known [113]. The $\bar{I}$ integrals read

$$
\begin{aligned}
\bar{I}_1 &= 2\overline{s_{j2}^2}+2\overline{s_{j2}}(e_1+e_2)+(2e_1e_2-e_3e_4)\overline{1}\,,\\
\bar{I}_2 &= -2\overline{s_{j2}^2}(e_{10})+2\overline{s_{j2}}(e_5e_{10}+e_9e_{10}-e_6e_7-e_8e_7)\\
&\quad+2\big((e_5e_6e_7+e_8e_9e_7-e_5e_9e_{10}-e_8e_6e_{11})\\
&\quad+e_3\left(e_{11}e_{10}-e_7^2\right)\big)\overline{1}\,,\\
\bar{I}_3 &= e_3\overline{1}\,,\\
\bar{I}_4 &= m_im_je_4\overline{1}\,,\\
\bar{I}_5 &= m_im_j\left(e_{10}e_{11}-e_7^2\right)\overline{1}\,,\\
\bar{I}_6 &= m_im_j\overline{1}\,,\\
\bar{I}_7 &= m_j(-e_{12}e_6)\overline{1}\,,\\
\bar{I}_8 &= m_i(e_{12}e_8)\overline{1}\,,\\
\bar{I}_9 &= m_j\left(\overline{s_{j2}}+(e_2)\overline{1}\right)\,,\\
\bar{I}_{10} &= m_i\left(\overline{s_{j2}}+(e_1)\overline{1}\right)\,,\\
\bar{I}_{11} &= -\overline{s_{j2}}(e_8-e_6)+(e_8e_9-e_5e_6)\overline{1}\,,
\end{aligned}
\tag{70}
$$

where

$$
\overline{s_{j2}^n}=\int_{s_{j2}^{\min}}^{s_{j2}^{\max}}\mathrm{d}s_{j2}s_{j2}^n\,. \tag{71}
$$

The quantities e_i read

$$
\begin{aligned}
e_1 &= -e_5-\frac{m_2-m_1}{s_{12}}e_8\,,\\
e_2 &= -e_9-\frac{m_2-m_1}{s_{12}}e_6\,,\\
e_3 &= \frac{1}{2}\left(m_i^2+m_j^2-s_{12}\right)\,,\\
e_4 &= e_{11}-\frac{\left(m_2^2-m_1^2\right)^2}{s_{12}}\,,\\
e_5 &= m_2^2+\frac{1}{2}\left(m_i^2+m_j^2-s_{12}\right)\,,\\
e_6 &= \frac{1}{2}\left(m_i^2-m_j^2+s_{12}\right)\,,\\
e_7 &= m_1^2-m_2^2\,,\\
e_8 &= \frac{1}{2}\left(m_i^2-m_j^2-s_{12}\right)\,,\\
e_9 &= m_1^2+\frac{1}{2}\left(m_i^2+m_j^2-s_{12}\right)\,,\\
e_{10} &= s_{12}\,,\\
e_{11} &= 2m_1^2+2m_2^2-s_{12}\,,\\
e_{12} &= -e_4\,.
\end{aligned}
\tag{72}
$$

4 Minimal SO(10) model and its predictions

Now we have all that is needed to find SL LFV processes: the description of the SUSY-breaking mechanism, the RGE equations connecting the GUT scale quantities with the weak-scale ones, the relevant interaction and mass parts of the MSSM Lagrangian with additional heavy neutrino fields, the effective Lagrangians of the processes considered at the MSSM level and the hadronization procedure for the quark currents. As explained in Sect. 2.1, in order to perform a concrete evaluation for the SL LFV processes, one needs information on the Dirac-neutrino Yukawa couplings (see Sect. 2.1). In this paper, we make use of the minimal SO(10) model to obtain them. We begin with an brief overview of the minimal SUSY-SO(10) model proposed in [77] and recently analyzed in detail in [78–87]. Even when we concentrate our discussion on the issue of how to reproduce the realistic fermion mass matrices in the SO(10) model, there are lots of possibilities for the introduction of Higgs multiplets. The minimal supersymmetric SO(10) model is the one in which only one **10** and one $\overline{\mathbf{126}}$ Higgs multiplet have Yukawa couplings (superpotential) with **16** matter multiplets. The quark and lepton mass matrices can be described as [77]

$$
\begin{aligned}
M_u &= c_{10}M_{10}+c_{126}M_{126}\,,\\
M_d &= M_{10}+M_{126}\,,\\
M_{\mathrm{D}} &= c_{10}M_{10}-3c_{126}M_{126}\,,\\
M_e &= M_{10}-3M_{126}\,,\\
M_{\mathrm{R}} &= c_{\mathrm{R}}M_{126}\,,
\end{aligned}
\tag{73}
$$

where M_u, M_d, M_{D}, M_e and M_{R} denote up-type quark, down-type quark, neutrino Dirac, charged-lepton and right-handed neutrino Majorana mass matrices, respectively. Note that all the quark and lepton mass matrices are characterized by only two basic mass matrices, M_{10} and M_{126}, and three complex coefficients c_{10}, c_{126} and c_{R}.

The mass matrix formulas in (73) lead to the GUT relation among quark and lepton mass matrices [77–82],

$$
M_e=c_d(M_d+\kappa M_u)\,, \tag{74}
$$

where

$$
c_d=-\frac{3c_{10}+c_{126}}{c_{10}-c_{126}}\,, \tag{75}
$$

$$
\kappa=-\frac{4}{3c_{10}+c_{126}}\,. \tag{76}
$$

Without loss of generality, one can start with the basis where M_u is real and diagonal, $M_u = D_u$. Since M_d is a symmetric matrix, it can be described as $M_d = V_{\rm CKM}^* D_d V_{\rm CKM}^\dagger$ by using the CKM matrix $V_{\rm CKM}$ and the real diagonal mass matrix D_d.[2] Considering the basis-independent quantities, $\mathrm{tr}[M_e^\dagger M_e]$, $\mathrm{tr}[(M_e^\dagger M_e)^2]$ and $\det[M_e^\dagger M_e]$, and eliminating $|c_d|$, one obtains two independent equations [78–82]:

$$\left(\frac{\mathrm{tr}[\widetilde{M_e}^\dagger \widetilde{M_e}]}{m_e^2+m_\mu^2+m_\tau^2}\right)^2 = \frac{\mathrm{tr}[(\widetilde{M_e}^\dagger \widetilde{M_e})^2]}{m_e^4+m_\mu^4+m_\tau^4}\,, \tag{77}$$

$$\left(\frac{\mathrm{tr}[\widetilde{M_e}^\dagger \widetilde{M_e}]}{m_e^2+m_\mu^2+m_\tau^2}\right)^3 = \frac{\det[\widetilde{M_e}^\dagger \widetilde{M_e}]}{m_e^2 m_\mu^2 m_\tau^2}\,, \tag{78}$$

where $\widetilde{M_e} \equiv V_{\rm CKM}^* D_d V_{\rm CKM}^\dagger + \kappa D_u$. With input data for six quark masses, three angles and one CP-phase in the CKM matrix and three charged-lepton masses, one can solve the above equations and determine κ and $|c_d|$. However, one parameter, the phase of c_d, is left undetermined [78–82]. The original basic mass matrices, M_{10} and M_{126}, are described by [78–82]

$$M_{10} = \frac{3+|c_d|e^{\mathrm{i}\sigma}}{4} V_{\rm CKM}^* D_d V_{\rm CKM}^\dagger + \frac{|c_d|e^{\mathrm{i}\sigma}\kappa}{4} D_u\,, \tag{79}$$

$$M_{126} = \frac{1-|c_d|\mathrm{e}^{\mathrm{i}\sigma}}{4} V_{\rm CKM}^* D_d V_{\rm CKM}^\dagger - \frac{|c_d|\mathrm{e}^{\mathrm{i}\sigma}\kappa}{4} D_u\,, \tag{80}$$

as functions of σ, the phase of c_d, with the solutions $|c_d|$ and κ, determined by the GUT relation.

The GUT relation (74) is valid only at the GUT scale. All quantities involved in the GUT relation have to be determined from the corresponding experimentally known quantities at the weak scale, RGE evolving them to the GUT scale. The experimental errors for the weak-scale quantities around their cental values [116] and phenomenologically constrained region of $\tan\beta$ [94] define the experimentally allowed region of input parameters.

Searching for the solution of the GUT relation is performed by sampling points in the parameter space, and checking whether (77) and (78) can be fulfilled [78–82]. The solution is not easy to find for several reasons. First, the number of free parameters of the minimal SO(10) model is almost the same as the number of input values (thirteen) [78–82]. Second, the solutions depend on the phases of fermion mass eigenvalues, which are undetermined by the diagonalization procedure. For simplicity, the masses are taken to be real, with a $-$ sign for m_u, m_c, m_d and m_s, and $+$ for m_t and m_b. Third, the solution of (77) and (78) is very sensitive to the input values and exists for a very restricted region in the parameter space. For the input values, we have taken the central experimental values for all three CKM angles and all quark masses except m_s and have varied $\tan\beta$, m_s and δ to find the solution. The solutions always appear in pairs, with approximately equal $(\kappa, |c_{\rm R}|)$ values. For a given $\tan\beta$ the solutions exist in a small region in the (m_s, δ) space of the bra (i.e. left angle, "⟨") shape, which is essentially the same for every $\tan\beta$ value. An example of such a region is given in Fig. 1 (black and green dots). The solutions of the GUT relation exist within the interval $2.019 \le \tan\beta \le 58.69$. At the boundary points the numerical instabilities characteristic for the CMSSM appear [94]).

To illustrate the characteristic values of the relevant parameters obtained numerically, we list them for the following values of the parameters: $\tan\beta = 45$, $m_s = 0.073$ and $\delta = 1.2$. One of the two solutions for $(\kappa, |c_{\rm R}|)$ is

$$\begin{aligned} \kappa &= 0.0133 - 0.000595\mathrm{i}\,, \\ |c_d| &= 7.065\,. \end{aligned} \tag{81}$$

For these values of varied parameters one obtains the following absolute values of the charged fermion masses (in units of GeV):

$$\begin{aligned} &m_u = 0.00103\,, \quad m_c = 0.299\,, \quad m_t = 133\,, \\ &m_d = 0.00170\,, \quad m_s = 0.0264\,, \quad m_b = 1.55\,, \\ &m_e = 0.000411\,, \quad m_\mu = 0.0868\,, \quad m_\tau = 1.69\,, \end{aligned}$$

and the CKM matrix (in the standard parametrization) is

$$V_{\rm CKM} = \begin{pmatrix} 0.975 & 0.222 & 0.000101 - 0.00261\mathrm{i} \\ -0.222 - 0.000113\mathrm{i} & 0.974 + 0.000121\mathrm{i} & 0.0320 \\ 0.00613 - 0.00254\mathrm{i} & -0.0314 - 0.000584\mathrm{i} & 0.999 \end{pmatrix},$$

at the GUT scale.

Once the parameters κ and $|c_d|$ are determined, one can describe all fermion mass matrices as a function of the phase σ, using (73), (79) and (80). The corresponding Yukawa matrices are determined, too. The right-handed neutrino mass matrix depends on the parameter $c_{\rm R}$, too. Therefore, the minimal-SO(10) model-light-Majorana-neutrino mass matrix, $M_\nu = -M_{\rm D}^{\rm T} M_{\rm R}^{-1} M_{\rm D}$, is a function of the phase σ and the parameter $c_{\rm R}$, too.

There is one comment in order. The bases of the u, d, e, D and R states are strongly correlated in the SO(10) phase (see (73)). In the MSSM phase, below the M_X scale, this correlation is lost, and the bases of these states can be chosen at will, up to the known low-energy constraints (e.g. the CKM relation for u and d states). In the following, the basis in which both the charged-lepton and right-handed Majorana-neutrino mass matrices are diagonal with real and positive eigenvalues at the GUT scale [70] is chosen.

The parameters σ and $c_{\rm R}$ are determined by fitting the neutrino oscillation data. RGE evolving the M_ν matrix to the weak scale [78–82, 117–120], and adjusting the neutrino oscillation data, one obtains the explicit values for σ and $c_{\rm R}$. The neutrino oscillation fit additionally constrains the parameter space of the GUT-relation solutions. Only part of the SO(10)-GUT-relation (SO(10)) solutions satisfies the neutrino oscillation-fit condition

[2] In general, $M_d = U^* D_d U^\dagger$ by using the general unitary matrix $U = \mathrm{e}^{\mathrm{i}\alpha}\mathrm{e}^{\mathrm{i}\beta T_3}\mathrm{e}^{\mathrm{i}\gamma T_8} V_{\rm CKM} \mathrm{e}^{\mathrm{i}\beta' T_3}\mathrm{e}^{\mathrm{i}\gamma' T_8}$. We omit the diagonal phases to keep the number of free parameters in the model as small as possible.

(NOFC) in the Fig. 1, too. They are represented by black regions in Fig. 1. It should be noted that the NOFC solutions exist for each value of $\tan\beta$. For small $\tan\beta$ values the region is larger and either touches the $\delta=\pi$ boundary of the (m_s,δ) parameter space or is close to it. For larger $\tan\beta$, it is smaller and closer to the $\delta=0$ boundary.

Turning back to the explicit values for the Yukawa matrices, for $\tan\beta=45$, $m_s=0.073$ and $\delta=1.2$ one obtains $\sigma=3.163$ [rad] and $c_{\mathrm{R}}=2.752\times10^{15}$, leading to the Dirac-neutrino Yukawa matrix,

$$Y_\nu = \begin{pmatrix} 0.000602+0.00391\mathrm{i} & -0.000937-0.000266\mathrm{i} & 0.0412+0.0513\mathrm{i} \\ 0.00483-0.0130\mathrm{i} & -0.0270-0.0478\mathrm{i} & 0.326+0.128\mathrm{i} \\ 0.00414-0.00144\mathrm{i} & 0.0564-0.0752\mathrm{i} & -0.353+0.584\mathrm{i} \end{pmatrix}. \tag{82}$$

To perform the MSSM-RGE [103,104] from the GUT scale to the weak scale, one has to know the MSSM-RGE initial values. These include Yukawa matrices which are now fixed, SUSY-breaking parameters and MSSM-Higgs parameters which are functions of the mSUGRA parameters m_0, $M_{1/2}$ and A_0, as well as the sign of the parameter μ defined in (4). The parameter A_0 is chosen to be equal to zero, because the parameters in the CMSSM weakly depend on its value [94,130]. The parameters m_0 and $M_{1/2}$ are chosen to fit the WMAP constraint on the cold dark matter (CDM) relic density [127,128],

$$\Omega_{\mathrm{CDM}}h^2=0.1126\,, \tag{83}$$

which can be transmuted into the approximate linear relation between m_0 and $M_{1/2}$ [129,130], with coefficients of the relation dependent on $\tan\beta$. For instance, for $\tan\beta=45$ and $A_0=0$

$$m_0\,[\mathrm{GeV}]=\frac{9}{28}M_{1/2}\,[\mathrm{GeV}]+150\,[\mathrm{GeV}]\,. \tag{84}$$

Further, the negative sign of μ, $\mu<0$, is chosen to obtain the MSSM contribution to the muon anomalous magnetic moment within the present experimental error (see below). There is only one mSUGRA parameter left undetermined. We took $M_{1/2}$ as the remaining free parameter.

With the initial conditions thus determined, one can solve the MSSM RGEs for all MSSM parameters evolving them from the GUT scale to the weak scale (they are also functions of the parameter $M_{1/2}$). Then one can find the masses, couplings and mixings for the SUSY particles. These data are used as an input into the formulas for the SL LFV amplitudes presented in previous sections. Notice that all masses at the weak scale functionally depend on the parameter $M_{1/2}$.

The SL LFV amplitudes depend on the parameters describing the hadronization of the hadron currents. Here is a list of the parameters we use. For the pseudoscalar meson decay constants, we take [113]

$$f_{\pi^0}=0.119\,[\mathrm{GeV}]\,,\quad f_\eta=0.131\,[\mathrm{GeV}]\,,\quad f_{\eta'}=0.118\,[\mathrm{GeV}]\,. \tag{85}$$

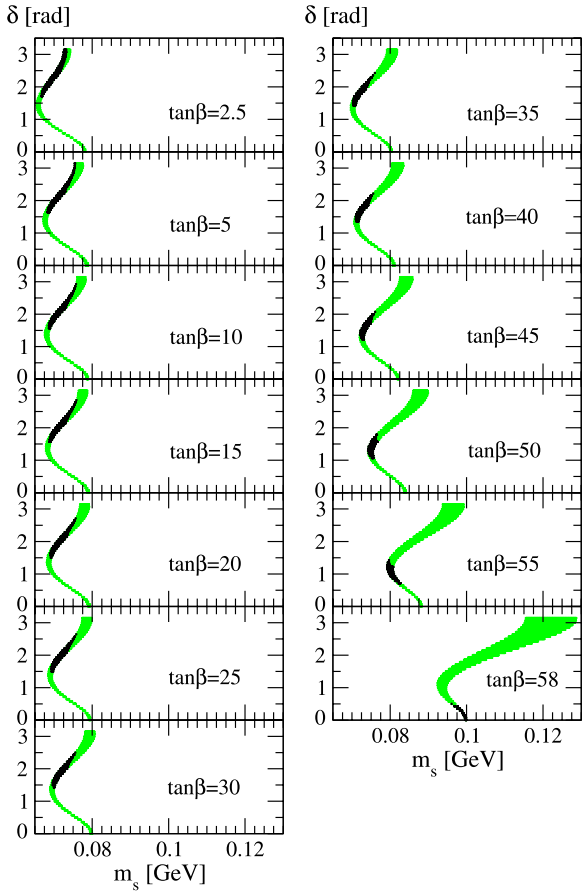

Fig. 1. The (m_s,δ) regions of SO(10) solutions, evaluated for $\tan\beta=2.5$, 5, 10, 15, 20, 25, 30, 35, 40, 45 and 50 are represented by *black* and *red regions*. The regions have the bra shape. The *black dots* represent SO(10) GUT-relation (SO(10)) solutions which satisfy the neutrino-oscillation-fit condition (NOFC). The SO(10)-NOFC solutions exist for each $\tan\beta$ value. For smaller $\tan\beta$ values, the SO(10)-NOFC-solutions' region is larger and closer to the case $\delta=\pi$, while for larger $\tan\beta$ values it is smaller and closer to the case $\delta=0$

For the vector-meson decay constants we use the values extracted from the vector-meson decay, $V\to e^+e^-$ [47],

$$\gamma_{\rho^0}=2.518\,,\quad \gamma_\phi=2.993\,,\quad \gamma_\omega=3.116\,. \tag{86}$$

The mixing angles between the singlet and octet states for the vector mesons and for the pseudoscalar mesons that we use are taken from [113]:

$$\theta_V=35^\circ\,,\quad \theta_P=-17.3^\circ\,. \tag{87}$$

In order to investigate the dependence of SL LFV branching ratios on the model parameters we plot their dependence on $m_{\tilde{\tau}_{\mathrm{R}}}$ and $\tan\beta$: for $\tau\to e\pi^0$, $\tau\to e\eta$, $\tau\to e\eta'$, $\tau\to\mu\pi^0$, $\tau\to\mu\eta$, and $\tau\to\mu\eta'$ in Fig. 2, for $\tau\to e\rho^0$, $\tau\to\mu\rho^0$, $\tau\to e\phi$, $\tau\to\mu\phi$, $\tau\to e\omega$, and $\tau\to\mu\omega$ in Fig. 3, for $\tau\to e\pi^+\pi^-$, $\tau\to\mu\pi^-\pi^+$, $\tau\to eK^0\overline{K}{}^0$, and $\tau\to\mu K^0\overline{K}{}^0$, $\tau\to eK^+K^-$, and $\tau\to\mu K^+K^-$, in Fig. 4, and for $\tau\to e\gamma$ and $\tau\to\mu\gamma$ in Fig. 5. The $\tan\beta=15,25,30,35,40,45$ and

50 are chosen because for these values the MSSM contribution to the anomalous magnetic moment assumes values smaller than the corresponding present experimental error $\Delta a_\mu^{\rm exp}\mu_{\rm B} = \frac{1}{2}(g_\mu - 2)\mu_{\rm B} = 7\times10^{-10}\,\mu_{\rm B}$ ($\mu_{\rm B}$ is the Bohr magneton) for $m_{\tilde\tau} < 400\,{\rm GeV}$ ($M_{1/2} < 1000\,{\rm GeV}$). $M_{1/2}$ values larger than 1000 GeV are not permitted by the WMAP constraint [129, 130]. As shown below and in Fig. 6, the region in which the curves are defined is determined by the condition $\Delta a_{\mu,{\rm MSSM}} < 7\times10^{-10}$.

In Fig. 6, the $m_{\tilde\tau_{\rm R}}$ and $\tan\beta$ dependence of the MSSM contribution to the anomalous magnetic moment $\Delta a_{\mu,{\rm MSSM}}$ and $B(\mu\to e\gamma)$ is shown. The points where the curves cross the experimental upper bounds (horizontal red lines in the figures) for the anomalous magnetic moment and $B(\mu\to e\gamma)$ (7×10^{-10} [131] and 1.2×10^{-11} [113], respectively) determine the boundary values of the $m_{\tilde\tau}$ mass that can be used in the evaluation of the LFV branching ratios. The intersections of the curves with the experimental bounds (red straight lines) are shown in small inserted panels. Starting from the left to the right, they correspond to $\tan\beta = 10$, 15, 20, 25, 30, 35, 40, 45, and 50 in the left panel ($B(\mu\to e\gamma)$) and to $\tan\beta = 50$ and 45, 40, 35, 30 and 15, and 25 in the right panel ($\Delta a_{\mu,{\rm MSSM}}$). Notice that the number of intersections in the right smaller panel is not equal to the number of curves. The reasons for that are the following: the $\Delta a_{\mu,{\rm MSSM}}$ curves for $\tan\beta = 50$ and 45 are very close and are represented by one intersection; the curves for $\tan\beta = 30$ and 15 cross and are also represented by one intersection; $\tan\beta = 10$ does not cross the 7×10^{-10} value at all, the $\tan\beta = 20$ curve crosses it

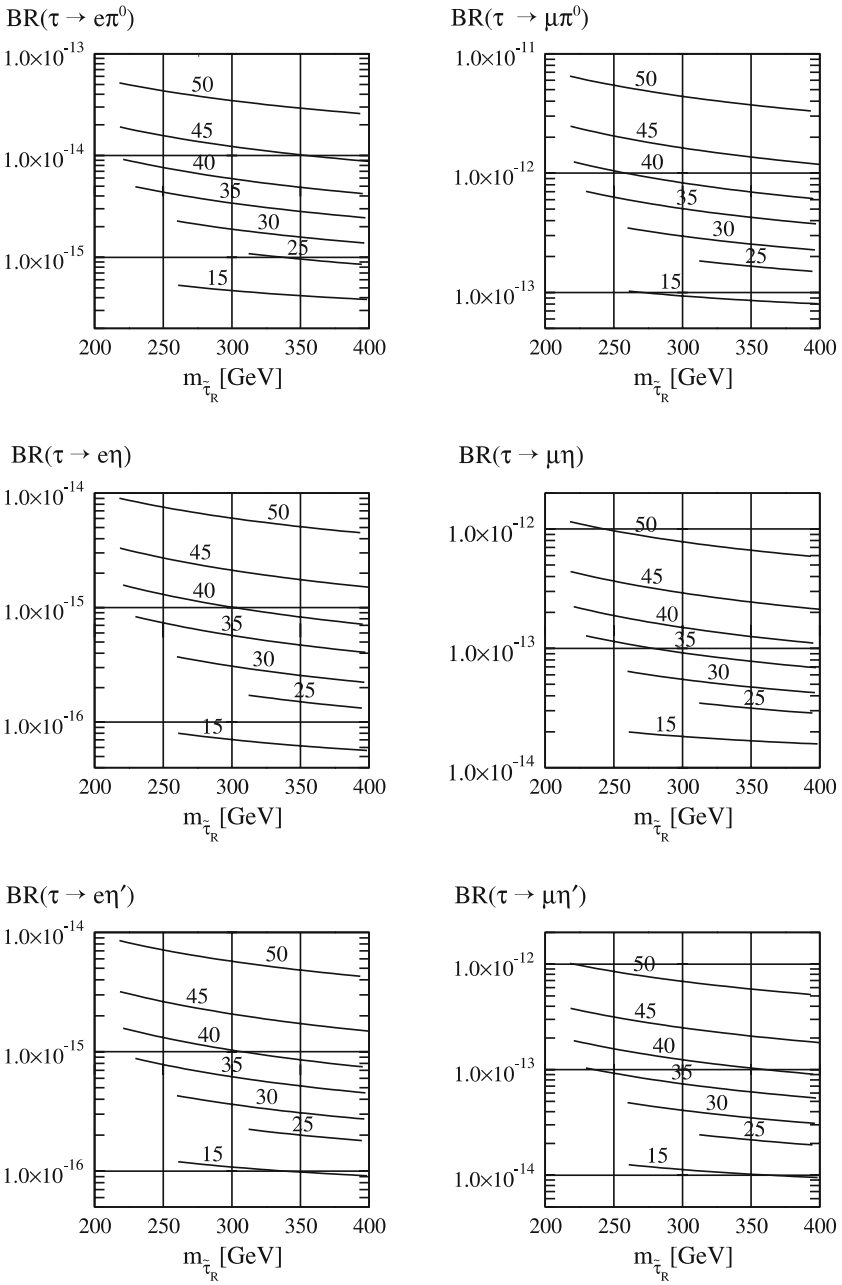

Fig. 2. The branching ratios for SL LFV decays $\tau\to e\pi^0/e\eta/e\eta'/\mu\pi^0/\mu\eta/\mu\eta'$ as a function of mass of the lightest charged sfermion $m_{\tilde\tau_{\rm R}}$. As input, we have taken $\tan\beta = 15$, 25, 30, 35, 40, 45, 50, $\mu < 0$, and $A_0 = 0$. The *curves* are in correspondence with the $\tan\beta$ values

above $m_{\tilde{\tau}} = 400\,\mathrm{GeV}$ ($M_{1/2} = 1000\,\mathrm{GeV}$). Notice that all $m_{\tilde{\tau}}$ boundaries determined by the $B(\mu \to e\gamma)$ are lower than the corresponding $\Delta a_{\mu,\mathrm{MSSM}}$ boundaries. Therefore, the latter give the lower bounds on the $m_{\tilde{\tau}}$ mass. Further, $\Delta a_{\mu,\mathrm{MSSM}}$ does not give the upper bound on the $m_{\tilde{\tau}}$ mass for any $\tan\beta$ value. Therefore, this model gives only the lower bound on the $m_{\tilde{\tau}}$ (or $M_{1/2}$) mass.

The theoretical upper bound for $\ell \to \ell'\gamma$ and SL LFV branching ratios for $\tan\beta = 30$, 35, 40, 45 and 50 are given in Table 1. The branching ratios for $\tan\beta = 15$ and 25 are not included for two reasons. First, their values are very small compared to the corresponding experimental upper bounds. Second, the regions of the allowed $M_{1/2}$ values for $\tan\beta = 15$ and 25 obtained from the WMAP constraint [129] do not have overlap with the corresponding regions of the model considered here. One can immediately notice that the SL LFV branching ratios of the τ lepton are too small compared to the present experimental upper bounds. On the other side, the $\ell \to \ell'\gamma$ branching ratios are much closer to the experimental upper bounds. Especially for $\tan\beta = 50$, $B(\tau \to \mu\gamma)$ exceeds the corresponding experimental upper-bound value.

To illustrate some general properties of the results given in Table 1 and Figs. 1–6, we again describe the results obtained for $\tan\beta = 45$. The maximal values for the branching ratios of the $\tau \to e/\mu\pi^0$ processes are found to be

$$\mathrm{BR}(\tau \to e\pi^0) \simeq 2.5 \times 10^{-14}, \tag{88}$$

$$\mathrm{BR}(\tau \to \mu\pi^0) \simeq 3.3 \times 10^{-12}, \tag{89}$$

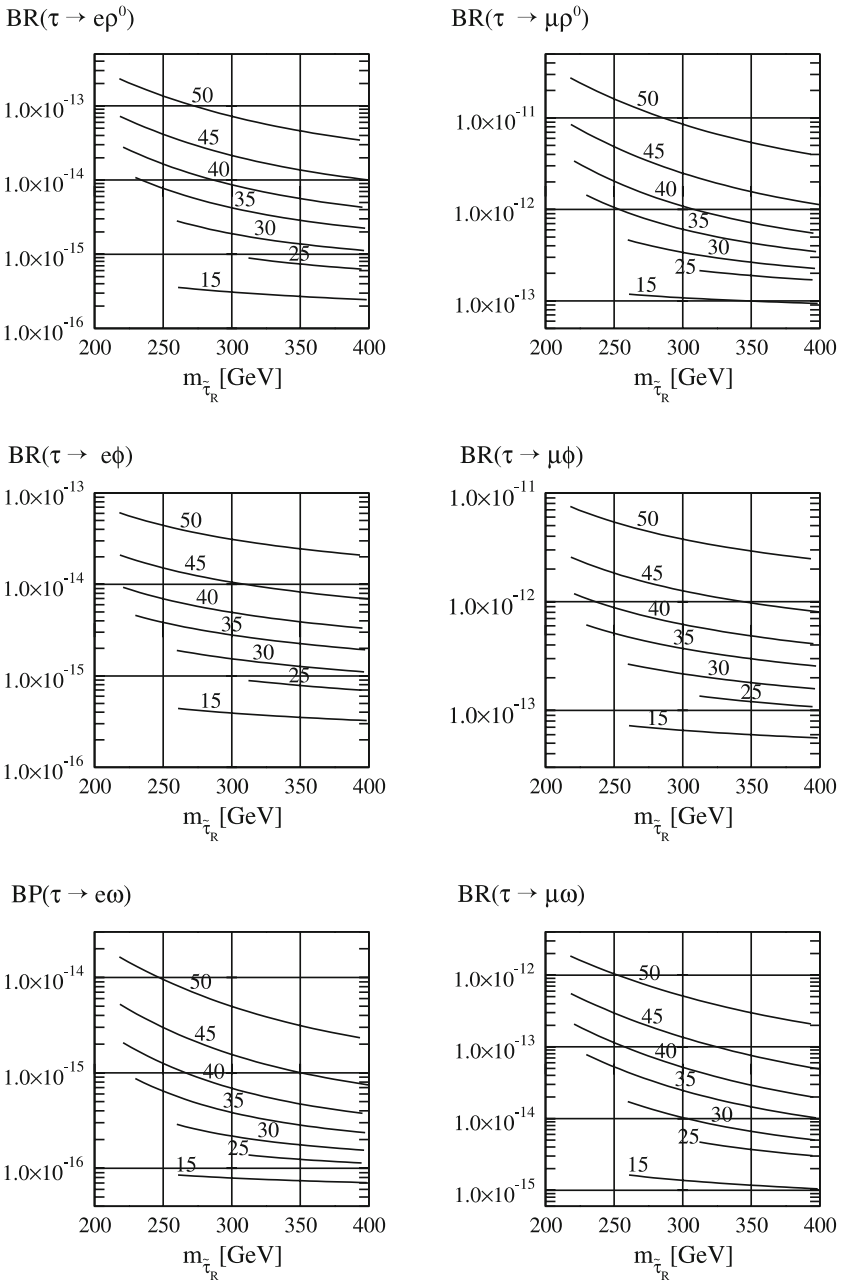

Fig. 3. The branching ratios for the SL LFV decays $\tau \to e\rho^0/e\phi/e\omega/\mu\rho^0/\mu\phi/\mu\omega$ as a function of mass of the lightest charged sfermion $m_{\tilde{\tau}_\mathrm{R}}$. The input parameters and line assignments are the same as in Fig. 2

and for the $\tau \to e/\mu\eta$ processes $\mathrm{BR}(\tau \to e/\mu\eta) \simeq 0.15 \times \mathrm{BR}(\tau \to e/\mu\pi^0)$. These values are obtained with the following set of parameters: $\tan\beta = 45$, $\mu < 0$, $A_0 = 0$, $M_{1/2} = 450\,[\mathrm{GeV}]$ and $m_0 = 295\,[\mathrm{GeV}]$. The parameters m_0 and $M_{1/2}$ (and A_0) satisfy the constraint (84). Therefore, the neutralino dark matter scenario can be realized. This parameter set also gives the MSSM contribution to the muon's $g-2$ within the range of the experimental error of the recent result of the Brookhaven E821 experiment [131]. It also provides the $\tau \to \mu\gamma$ and $\mu \to e\gamma$ branching ratios close to the current experimental bound [43]. The ratio between the two processes $\tau \to e/\mu\pi^0$ and $\tau \to e/\mu\eta$ is the result of the dominance of the Z-boson-penguin amplitude in these processes, and it reflects the difference in the form factors and the mixings between the singlet state and the octet state of the η mesons,

$$\frac{\mathrm{BR}(\tau \to e/\mu\eta)}{\mathrm{BR}(\tau \to e/\mu\pi)} \sim \left(\frac{f_\eta}{f_\pi}\right)^2 \times \left(\frac{c_P}{\sqrt{3}} + \frac{s_P}{\sqrt{6}}\right)^2 \sim 0.15\,. \tag{90}$$

We can also see the correlation between the branching ratios for the processes $\tau \to e/\mu\rho^0$ and $\tau \to e/\mu\gamma$ as $\mathrm{BR}(\tau \to e/\mu\rho^0) \simeq 3.2 \times 10^{-3} \times \mathrm{BR}(\tau \to e/\mu\gamma)$. The estimate of this ratio based on the assumption of photon-penguin-amplitude dominance in these amplitudes gives the result

$$\frac{\mathrm{BR}(\tau \to e/\mu\rho^0)}{\mathrm{BR}(\tau \to e/\mu\gamma)} \sim \frac{1}{2}\left(\frac{e}{\gamma_{\rho^0}}\right)^2 \sim 7 \times 10^{-3}\,. \tag{91}$$

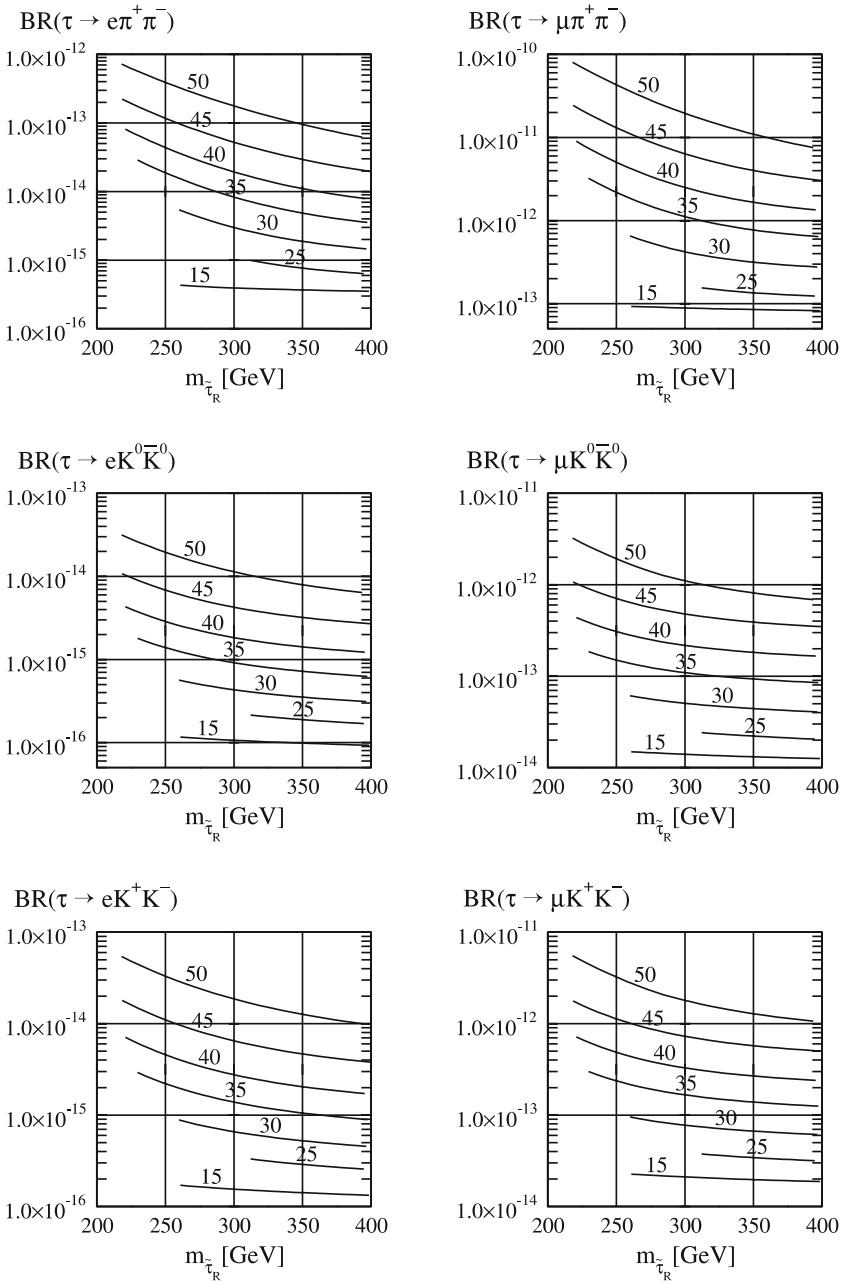

Fig. 4. The branching ratios for the SL LFV decays $\tau \to e\pi^+\pi^-/eK^0\overline{K}^0/eK^+K^-/\mu\pi^+\pi^-/\mu K^+K^-/\mu K^0\overline{K}^0$ as a function of the mass of the lightest charged sfermion $m_{\tilde{\tau}_\mathrm{R}}$. The input parameters and line assignments are the same as in Fig. 2

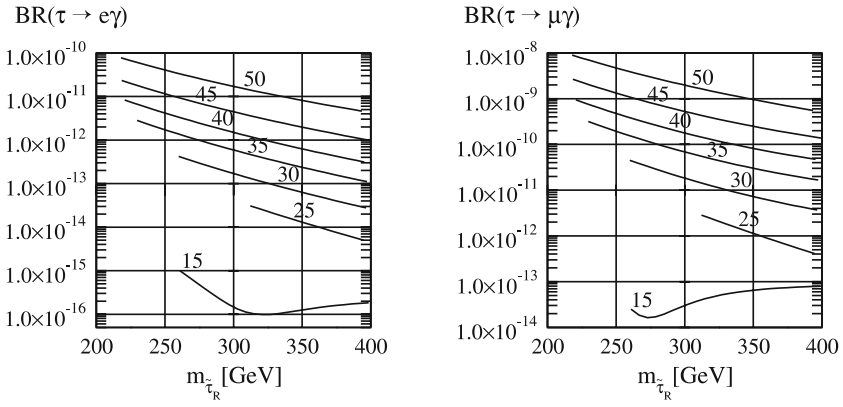

Fig. 5. The branching ratios for the decays $\tau \to e\gamma/\mu\gamma$ as a function of mass of the lightest charged sfermion $m_{\tilde{\tau}_{\rm R}}$. The input parameters and line assignments are the same as in Fig. 2

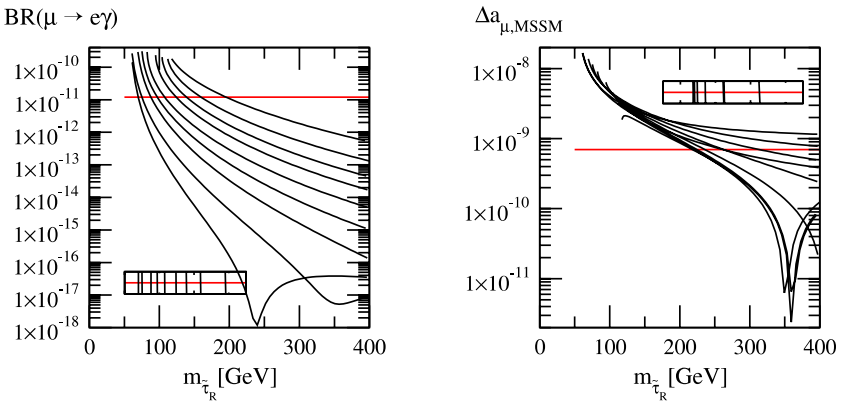

Fig. 6. The anomalous magnetic moment and branching ratio for $\mu \to e\gamma$ as a function of mass of the lightest charged sfermion $m_{\tilde{\tau}_{\rm R}}$. These quantities restrict the region of $m_{\tilde{\tau}_{\rm R}}$ values. The present experimental upper limits are represented by *horizontal red lines*. The *small inserted panels* represent the part of the corresponding figures very close to the *horizontal red lines* with no enlargement in the x-direction and very strongly stretched in the y-direction. They show where the curves in the large figures cross the experimental-bound value. Starting from left to right the crossings in the *left (right)* panel correspond to $\tan\beta = 10$, 15, 20, 25, 20, 35, 40, 45 and 50 ($\tan\beta = 50$ and 45, 40, 35, 30 and 15, 25)

This shows that the Z-boson-penguin amplitude is comparable in magnitude to the photon-penguin amplitude. When we impose the constraints from the recent muon's $g-2$ measurements [131] and from the upper limits on the $\mu \to e\gamma$ branching ratio [113], we obtain the result that the model permits the $m_{\tilde{\tau}_{\rm R}}$ values satisfying

$$m_{\tilde{\tau}_{\rm R}} > 218\,[\text{GeV}]\,. \tag{92}$$

As explained, the lower bound comes from the muonic $g-2$ constraint. The lower bound from the $\mu \to e\gamma$ branching ratio is below the lower bound from the muon's $g-2$ constraint. The $g-2$ curve has an uprising behavior above $m_{\tilde{\tau}_{\rm R}} = 350$ [GeV], but at $m_{\tilde{\tau}_{\rm R}} = 1000$ [GeV] ($M_{1/2} = 2200$ [GeV]) it is almost independent on $m_{\tilde{\tau}_{\rm R}}$ and has a value 5.3×10^{-10}, slightly below the present experimental $g-2$ uncertainty (the corresponding $\tan\beta = 15$, 25, 30, 35, 40, 45, 50 curves show the same type of behavior). Therefore, one can expect that the improvement of the $g-2$ measurements will give the upper limit on $m_{\tilde{\tau}_{\rm R}}$, too. Using the lower bound on $m_{\tilde{\tau}_{\rm R}}$ values, one can find the theoretical upper bounds for all leptonic and SL LFV branching ratios.

5 Summary

The evidence for the neutrino masses and flavor mixings implies the non-conservation of the lepton-flavor symmetry. Thus, the LFV processes in the charged-lepton sector are expected. In the supersymmetric model based on the minimal SO(10) model, the values for the rates of the LFV processes are generally still several orders of magnitudes below the accessible current experimental bounds. In this paper, we have presented the detailed theoretical description for the SL LFV decays of the charged leptons with one or two pseudoscalar mesons or one vector meson in the final state. Also, some previous formulas have been corrected. The γ-penguin amplitude is corrected to assure gauge invariance, the Z-penguin amplitude is corrected, new contributions to the box amplitude have been found and previously neglected terms are given.

To evaluate the decay rates of the LFV processes within the MSSM, the parameters and the LFV interactions of the MSSM have to be specified. It has been shown [78–82] that the minimal SUSY-SO(10) model can simultaneously accommodate all observed quark–lepton mass matrix data involving the neutrino oscillation data with appropriately fixed free parameters. Here we show that it can be done for any value of $\tan\beta$ (Fig. 1). In the SUSY-SO(10) model, the Dirac-neutrino Yukawa coupling matrix is completely determined, and its off-diagonal components are the primary source of the lepton-flavor violation in the basis where the charged-lepton and the right-handed neutrino mass matrices are real and diagonal. Using this Yukawa coupling matrix, we have calculated the rate of the LFV processes assuming the mSUGRA scenario. The analytical formulas of various SL LFV processes, $\ell_i \to \ell_j P$,

Table 1. Theoretical upper bounds (T.u.b.) $\ell \to \ell'\gamma$ processes and dominant SL LFV processes. The upper bounds are obtained at the lower $m_{\tilde{\tau}}$ values, obtained from the muonic $g-2$ constraint. We quote the experimental data (E.u.b) mainly from [121–126] and partly from [113]

Process	T.u.b.					E.u.b.
	30	35	40	45	50	
$\mu \to e\gamma$	6.3×10^{-14}	3.6×10^{-13}	9.8×10^{-13}	2.5×10^{-12}	7.4×10^{-12}	1.2×10^{-11} [113]
$\tau \to e\gamma$	4.2×10^{-13}	2.8×10^{-12}	8.3×10^{-12}	2.3×10^{-11}	7.8×10^{-11}	1.1×10^{-7} [124–126]
$\tau \to \mu\gamma$	4.5×10^{-11}	3.2×10^{-10}	9.4×10^{-10}	2.7×10^{-9}	9.0×10^{-9}	6.8×10^{-8} [124–126]
$\tau \to e\pi^0$	2.3×10^{-15}	4.9×10^{-15}	9.2×10^{-15}	1.9×10^{-14}	5.2×10^{-14}	1.9×10^{-7} [121, 122]
$\tau \to \mu\pi^0$	3.5×10^{-13}	7.0×10^{-13}	1.2×10^{-12}	2.5×10^{-12}	6.5×10^{-12}	4.3×10^{-7} [121, 122]
$\tau \to e\eta$	3.7×10^{-16}	8.3×10^{-16}	1.6×10^{-15}	3.3×10^{-15}	9.0×10^{-15}	2.3×10^{-7} [121, 122]
$\tau \to \mu\eta$	6.4×10^{-14}	1.3×10^{-13}	2.2×10^{-13}	4.4×10^{-13}	1.2×10^{-12}	2.3×10^{-7} [121, 122]
$\tau \to e\eta'$	4.3×10^{-16}	8.8×10^{-16}	1.6×10^{-15}	3.2×10^{-15}	8.5×10^{-15}	10×10^{-7} [121, 122]
$\tau \to \mu\eta'$	4.9×10^{-14}	1.0×10^{-13}	1.9×10^{-13}	3.8×10^{-13}	1.0×10^{-12}	4.1×10^{-7} [121, 122]
$\tau \to e\rho^0$	2.8×10^{-15}	1.1×10^{-14}	2.8×10^{-14}	7.3×10^{-14}	2.3×10^{-13}	2.0×10^{-6} [113]
$\tau \to \mu\rho^0$	4.6×10^{-13}	1.4×10^{-12}	3.4×10^{-12}	8.5×10^{-12}	2.8×10^{-12}	6.3×10^{-6} [113]
$\tau \to e\phi$	1.9×10^{-15}	4.6×10^{-15}	9.3×10^{-15}	2.1×10^{-14}	6.1×10^{-14}	6.9×10^{-6} [113]
$\tau \to \mu\phi$	2.7×10^{-13}	6.1×10^{-13}	1.2×10^{-12}	2.6×10^{-12}	7.5×10^{-12}	7.0×10^{-6} [113]
$\tau \to e\omega$	2.9×10^{-16}	8.7×10^{-16}	2.7×10^{-15}	5.2×10^{-15}	1.6×10^{-14}	–
$\tau \to \mu\omega$	1.7×10^{-14}	7.8×10^{-14}	2.1×10^{-13}	5.5×10^{-13}	1.8×10^{-12}	–
$\tau \to e\pi^+\pi^-$	5.4×10^{-15}	2.9×10^{-14}	8.1×10^{-14}	2.2×10^{-13}	7.2×10^{-13}	8.7×10^{-7} [123]
$\tau \to \mu\pi^+\pi^-$	6.6×10^{-13}	3.2×10^{-12}	8.9×10^{-12}	2.4×10^{-11}	8.0×10^{-11}	2.8×10^{-7} [123]
$\tau \to eK^0\overline{K}^0$	5.6×10^{-16}	1.8×10^{-15}	4.3×10^{-15}	1.1×10^{-14}	3.2×10^{-14}	2.2×10^{-6} [113]
$\tau \to \mu K^0\overline{K}^0$	6.1×10^{-14}	1.9×10^{-13}	4.4×10^{-13}	1.1×10^{-12}	3.2×10^{-12}	3.4×10^{-6} [113]
$\tau \to eK^+K^-$	8.8×10^{-16}	2.9×10^{-15}	7.1×10^{-15}	1.8×10^{-14}	5.4×10^{-14}	3.0×10^{-7} [123]
$\tau \to \mu K^+K^-$	9.5×10^{-14}	3.0×10^{-13}	7.2×10^{-13}	1.8×10^{-12}	5.5×10^{-12}	11.7×10^{-7} [123]

$\ell_i \to \ell_j V$ and $\ell_i \to \ell_j PP$, are given. Using these formulas, we have numerically evaluated the $\ell_i \to \ell_j P$, $\ell_i \to \ell_j V$ and $\ell_i \to \ell_j P_1 P_2$ branching ratios. Among these, only the branching ratio of $\tau \to \mu\gamma$ is close to the present experimental value [124–126], while $\tau \to e\gamma$ might be interesting for the near future experiments [132]. The typical CMSSM parameters used in the calculations are assumed to realize the neutralino dark matter scenario consistent with the WMAP data.

Acknowledgements. A.I. would like to thank to I. Picek and S. Fajfer for the discussions on current-quark masses and evaluation of tensor-quark current. A part of the work was presented by A.I. at the workshop, "The 8th International Workshop on Tau-Lepton Physics (Tau04)", held in Nara-ken New Public Hall, Japan. We are grateful to all organizers of this workshop and particularly to Prof. Ohshima for his kind hospitality extended to A.I and T.K. during their stay at Nagoya University. T.F. would like to thank S.T. Petcov for his hospitality at SISSA. The work of T.F. was supported by the Grant in Aid for Scientific Research from the Ministry of Education, Science and Culture (# 16540269). T.K. would like to thank K.S. Babu for his hospitality at Oklahoma State University. The work of T.K. is supported by the Research Fellowship of the Japan Society for the Promotion of Science (#1911329). The work of A.I is supported by the Ministry of Science and Technology of Republic of Croatia under contract 0119261.

Appendix A: Notation for the MSSM Lagrangian

Here we summarize our notation, necessary for defining the masses of the sparticles in the MSSM Lagrangian. The vacuum expectation values of the MSSM Higgs fields satisfy

$$v \equiv \sqrt{\langle H_u^0\rangle^2 + \langle H_d^0\rangle^2} = 174.1\,[\mathrm{GeV}]\,, \tag{A.1}$$

and

$$\tan\beta \equiv \frac{\langle H_u^0\rangle}{\langle H_d^0\rangle}\,. \tag{A.2}$$

The charged fermion mass matrices are given by

$$M_u^{ij} = -Y_u^{ij} v \sin\beta\,, \tag{A.3}$$
$$M_d^{ij} = Y_d^{ij} v \cos\beta\,, \tag{A.4}$$
$$M_e^{ij} = Y_e^{ij} v \cos\beta\,. \tag{A.5}$$

The chargino mass matrix is written

$$\mathcal{L} = -(\overline{\widetilde{W}_{\mathrm{R}}^-},\quad \overline{\widetilde{H}_{u\mathrm{R}}^-})\,,\quad M_{\tilde{\chi}^\pm}\begin{pmatrix}\widetilde{W}_{\mathrm{L}}^- \\ \widetilde{H}_{d\mathrm{L}}^-\end{pmatrix} + \mathrm{h.c.}\,,$$
$$M_{\tilde{\chi}^\pm} = \begin{pmatrix} M_2 & \sqrt{2}M_W\cos\beta \\ \sqrt{2}M_W\sin\beta & \mu\end{pmatrix}\,. \tag{A.6}$$

The neutralino mass matrix is

$$\mathcal{L} = -\frac{1}{2}\left(\widetilde{B}_{\rm L},\ \widetilde{W}^3_{\rm L},\ \widetilde{H}^0_{d{\rm L}},\ \widetilde{H}^0_{u{\rm L}}\right),$$
$$M_{\tilde{\chi}^0}\begin{pmatrix}\widetilde{B}_{\rm L}\\ \widetilde{W}^3_{\rm L}\\ \widetilde{H}^0_{d{\rm L}}\\ \widetilde{H}^0_{u{\rm L}}\end{pmatrix} + {\rm h.c.},$$
$$M_{\tilde{\chi}^0} = \begin{pmatrix} M_1 & 0 & -M_Z s_{\rm W}\cos\beta & M_Z s_{\rm W}\sin\beta \\ 0 & M_2 & M_Z c_{\rm W}\cos\beta & -M_Z c_{\rm W}\sin\beta \\ -M_Z s_{\rm W}\cos\beta & M_Z c_{\rm W}\cos\beta & 0 & -\mu \\ M_Z s_{\rm W}\sin\beta & -M_Z c_{\rm W}\sin\beta & -\mu & 0 \end{pmatrix}. \tag{A.7}$$

The squark mass matrices are written

$$\mathcal{L} = -\left(m^2_{\tilde{u}}\right)^{ij}\tilde{u}^\dagger_i\tilde{u}_j - \left(m^2_{\tilde{d}}\right)^{ij}\tilde{d}^\dagger_i\tilde{d}_j,$$
$$m^2_{\tilde{u}} = \begin{pmatrix} m^2_{\tilde{q}} + M_u^\dagger M_u & -A_u^\dagger v\sin\beta - M_u^\dagger\mu^*\cot\beta \\ -A_u v\sin\beta - M_u\mu\cot\beta & m^2_{\tilde{u}} + M_u M_u^\dagger - M_Z^2\cos 2\beta s^2_{\rm W}\end{pmatrix} + \begin{pmatrix} M_Z^2\cos 2\beta\left(\frac{1}{2} - \frac{2}{3}s^2_{\rm W}\right)\mathbf{1}_{3\times3} & 0 \\ 0 & \frac{2}{3}M_Z^2\cos 2\beta s^2_{\rm W}\mathbf{1}_{3\times3}\end{pmatrix},$$
$$m^2_{\tilde{d}} = \begin{pmatrix} m^2_{\tilde{q}} + M_d^\dagger M_d & A_d^\dagger v\cos\beta - M_d^\dagger\mu^*\tan\beta \\ A_d v\cos\beta - M_d\mu\tan\beta & m^2_{\tilde{d}} + M_d M_d^\dagger - M_Z^2\cos 2\beta s^2_{\rm W}\end{pmatrix} + \begin{pmatrix} M_Z^2\cos 2\beta\left(-\frac{1}{2} + \frac{1}{3}s_{\rm W}\right)\mathbf{1}_{3\times3} & 0 \\ 0 & -\frac{1}{3}M_Z^2\cos 2\beta s^2_{\rm W}\mathbf{1}_{3\times3}\end{pmatrix}. \tag{A.8}$$

The slepton mass matrices read

$$\mathcal{L} = -(m^2_{\tilde{\nu}})^{ij}\tilde{\nu}^\dagger_i\tilde{\nu}_j - (m^2_{\tilde{e}})^{ij}\tilde{e}^\dagger_i\tilde{e}_j,$$
$$m^2_{\tilde{\nu}} = m^2_{\tilde{\ell}} + \frac{1}{2}M_Z^2\cos 2\beta\mathbf{1}_{3\times3},$$
$$m^2_{\tilde{e}} = \begin{pmatrix} m^2_{\tilde{\ell}} + M_e^\dagger M_e & A_e^\dagger v\cos\beta - M_e^\dagger\mu^*\tan\beta \\ A_e v\cos\beta - M_e\mu\tan\beta & m^2_{\tilde{e}} + M_e M_e^\dagger - M_Z^2\cos 2\beta s^2_{\rm W}\end{pmatrix} + \begin{pmatrix} M_Z^2\cos 2\beta\left(-\frac{1}{2} + s^2_{\rm W}\right)\mathbf{1}_{3\times3} & 0 \\ 0 & -M_Z^2\cos 2\beta s^2_{\rm W}\mathbf{1}_{3\times3}\end{pmatrix}. \tag{A.9}$$

They are diagonalized by unitary matrices as follows:

$$O_{\rm R}M_{\tilde{\chi}^\pm}O_{\rm L}^\dagger = {\rm diag}\left(M_{\tilde{\chi}^-_1}, M_{\tilde{\chi}^-_2}\right),$$
$$O_N^* M_{\tilde{\chi}^0}O_N^\dagger = {\rm diag}\left(M_{\tilde{\chi}^0_1}, M_{\tilde{\chi}^0_2}, M_{\tilde{\chi}^0_3}, M_{\tilde{\chi}^0_4}\right),$$
$$U_{\tilde{f}}m^2_{\tilde{f}}U^\dagger_{\tilde{f}} = {\rm diag}\left(m^2_{\tilde{f}_1}, \ldots, m^2_{\tilde{f}_6}\right) \quad (f = u, d, e),$$
$$U_{\tilde{\nu}}m^2_{\tilde{\nu}}U^\dagger_{\tilde{\nu}} = {\rm diag}\left(m^2_{\tilde{\nu}_1}, m^2_{\tilde{\nu}_2}, m^2_{\tilde{\nu}_3}\right). \tag{A.10}$$

Appendix B: Lagrangian for fermion–sfermion–gaugino/Higgsino interactions in MSSM

The LFV interactions in the MSSM include the fermion–sfermion–gaugino/Higgsino vertices. These vertices, and the corresponding coupling constants ($C^{{\rm L,R}(f)}_{iAX}$, $N^{{\rm L,R}(f)}_{iAX}$, $f = \nu, e, u, d$) are defined by the following Lagrangian:

$$\begin{aligned}
\mathcal{L} = {} & \bar{u}_i\left[C^{{\rm L}(u)}_{iAX}P_{\rm L} + C^{{\rm R}(u)}_{iAX}P_{\rm R}\right]\widetilde{\chi}^+_A\widetilde{d}_X \\
& + \bar{d}_i\left[C^{{\rm L}(d)}_{iAX}P_{\rm L} + C^{{\rm R}(d)}_{iAX}P_{\rm R}\right]\widetilde{\chi}^-_A\widetilde{u}_X \\
& + \bar{\nu}_i C^{{\rm R}(\nu)}_{iAX}P_{\rm R}\widetilde{\chi}^+_A\widetilde{e}_X + \bar{e}_i\left[C^{{\rm L}(e)}_{iAX}P_{\rm L} + C^{{\rm R}(e)}_{iAX}P_{\rm R}\right]\widetilde{\chi}^-_A\widetilde{\nu}_X \\
& + \bar{u}_i\left[N^{{\rm L}(u)}_{iAX}P_{\rm L} + N^{{\rm R}(u)}_{iAX}P_{\rm R}\right]\widetilde{\chi}^0_A\widetilde{u}_X \\
& + \bar{d}_i\left[N^{{\rm L}(d)}_{iAX}P_{\rm L} + N^{{\rm R}(d)}_{iAX}P_{\rm R}\right]\widetilde{\chi}^0_A\widetilde{d}_X \\
& + \bar{\nu}_i N^{{\rm R}(\nu)}_{iAX}P_{\rm R}\widetilde{\chi}^0_A\widetilde{\nu}_X + \bar{e}_i\left[N^{{\rm L}(e)}_{iAX}P_{\rm L} + N^{{\rm R}(e)}_{iAX}P_{\rm R}\right]\widetilde{\chi}^0_A\widetilde{e}_X \\
& + {\rm h.c.} \\
\equiv {} & \overline{u}_i P_{\rm L}\tilde{\chi}^+_A\tilde{d}_X\left[g\left\{-\frac{m_{u_i}}{\sqrt{2}M_W\sin\beta}(O_{\rm R})_{A2}(U^*_{\tilde{d}})_{Xi}\right\}\right] \\
& + \overline{u}_i P_{\rm R}\tilde{\chi}^+_A\tilde{d}_X\left[g\left\{(O_{\rm L})_{A1}(U^*_{\tilde{d}})_{Xi} + \frac{m_{d_k}}{\sqrt{2}M_W\cos\beta}\right.\right. \\
& \left.\left.\times(V_{\rm CKM})_{kj}(V^*_{\rm CKM})_{ki}(O_{\rm L})_{A2}(U^*_{\tilde{d}})_{X,j+3}\right\}\right] \\
& + \overline{d}_i P_{\rm L}\tilde{\chi}^-_A\tilde{u}_X\left[g\left\{\frac{m_{d_i}}{\sqrt{2}M_W\cos\beta}(O^*_{\rm L})_{A2}(U^*_{\tilde{u}})_{Xj}\right\}\right. \\
& \left.\times(V_{\rm CKM})_{ij}\right] \\
& + \overline{d}_i P_{\rm R}\tilde{\chi}^-_A\tilde{u}_X\left[g\left\{(O^*_{\rm R})_{A1}(U^*_{\tilde{u}})_{Xj} - \frac{m_{u_j}}{\sqrt{2}M_W\sin\beta}\right.\right. \\
& \left.\left.\times(O^*_{\rm R})_{A2}(U^*_{\tilde{u}})_{X,j+3}\right\}(V^*_{\rm CKM})_{ij}\right] \\
& + \overline{\nu}_i P_{\rm R}\tilde{\chi}^+_A\tilde{e}_X\left[g\left\{(O_{\rm L})_{A1}(U^*_{\tilde{e}})_{Xj} + \frac{m_{e_i}}{\sqrt{2}M_W\cos\beta}\right.\right. \\
& \left.\left.\times(O_{\rm L})_{A2}(U^*_{\tilde{e}})_{X,j+3}\right\}(U^*_{\rm MNS})_{ij}\right] \\
& + \overline{e}_i P_{\rm L}\tilde{\chi}^-_A\tilde{\nu}_X\left[g\left\{\frac{m_{e_i}}{\sqrt{2}M_W\cos\beta}(O^*_{\rm L})_{A\,2}(U^*_{\tilde{\nu}})_{Xi}\right\}\right] \\
& + \overline{e}_i P_{\rm R}\tilde{\chi}^-_A\tilde{\nu}_X\left[g\left\{(O^*_{\rm R})_{A1}(U^*_{\tilde{\nu}})_{Xi}\right\}\right] \\
& + \overline{u}_i P_{\rm L}\tilde{\chi}^0_A\tilde{u}_X\left[\frac{g}{\sqrt{2}}\left\{\frac{m_{u_i}}{M_W\sin\beta}(O^*_N)_{A4}(U^*_{\tilde{u}})_{Xi}\right.\right. \\
& \left.\left.\times -\frac{4}{3}\tan\theta_{\rm W}(O^*_N)_{A1}(U^*_{\tilde{u}})_{X,i+3}\right\}\right] \\
& + \overline{u}_i P_{\rm R}\tilde{\chi}^0_A\tilde{u}_X\left[\frac{g}{\sqrt{2}}\left\{\frac{m_{u_i}}{M_W\sin\beta}(O_N)_{A4}(U^*_{\tilde{u}})_{X,i+3}\right.\right. \\
& \left.\left.+\left[(O_N)_{A2} + \frac{1}{3}\tan\theta_{\rm W}(O_N)_{A1}\right](U^*_{\tilde{u}})_{Xi}\right\}\right] \\
& + \overline{d}_i P_{\rm L}\tilde{\chi}^0_A\tilde{d}_X\left[\frac{g}{\sqrt{2}}\left\{-\frac{m_{d_i}}{M_W\cos\beta}(O^*_N)_{A3}(U^*_{\tilde{d}})_{Xj}\right.\right. \\
& \left.\left.+\frac{2}{3}\tan\theta_{\rm W}(O^*_N)_{A1}(U^*_{\tilde{d}})_{X,j+3}\right\}(V_{\rm CKM})_{ij}\right]
\end{aligned}$$

$$
\begin{aligned}
&+\overline{d}_i P_{\mathrm{R}} \tilde{\chi}^0_A \tilde{d}_X \left[\frac{g}{\sqrt{2}}\left\{-\frac{m_{d_i}}{M_W \cos\beta}(O_N)_{A3}(U^*_{\tilde{d}})_{X,j+3}\right.\right.\\
&\left.\left.+\left[-(O_N)_{A2}+\frac{1}{3}\tan\theta_{\mathrm{W}}(O_N)_{A1}\right](U^*_{\tilde{d}})_{Xj}\right\}(V_{\mathrm{CKM}})_{ij}\right]\\
&+\overline{\nu}_i P_{\mathrm{R}} \tilde{\chi}^0_A \tilde{\nu}_X \left[\frac{g}{\sqrt{2}}\left[(O_N)_{A2}-\tan\theta_{\mathrm{W}}(O_N)_{A1}\right]\right.\\
&\left.\times(U^*_{\tilde{\nu}})_{X,j}(U_{\mathrm{MNS}})_{ij}\right]\\
&+\overline{e}_i P_{\mathrm{L}} \tilde{\chi}^0_A \tilde{e}_X \left[\frac{g}{\sqrt{2}}\left\{-\frac{m_{e_i}}{M_W \cos\beta}(O^*_N)_{A3}(U^*_{\tilde{e}})_{Xi}\right.\right.\\
&\left.\left.\times+2\tan\theta_{\mathrm{W}}(O^*_N)_{A1}(U^*_{\tilde{e}})_{X,i+3}\right\}\right]\\
&+\overline{e}_i P_{\mathrm{R}} \tilde{\chi}^0_A \tilde{e}_X \left[\frac{g}{\sqrt{2}}\left\{-\frac{m_{e_i}}{M_W \cos\beta}(O_N)_{A3}(U^*_{\tilde{e}})_{X,i+3}\right.\right.\\
&\left.\left.+\left[-(O_N)_{A2}-\tan\theta_{\mathrm{W}}(O_N)_{A1}\right](U^*_{\tilde{e}})_{Xi}\right\}\right]\\
&+\mathrm{h.c.}\,, \qquad \text{(B.1)}
\end{aligned}
$$

where U_{MNS} is the Maki–Nakagawa–Sakata matrix. The rest of the notation either has been defined before or is the same as in [70].

Appendix C: Trilinear interactions of fermions or bosons with Z^0-boson or photon

The interactions of the Z^0-boson or photon with any fermion or any boson follow from the $\mathrm{SU}(2)_{\mathrm{L}} \times \mathrm{U}(1)_Y$ gauge symmetry. We have

$$
\mathcal{L}_f = -g \sum_f \overline{f}\left[\not{Z}\left(I_3^f \frac{1}{c_{\mathrm{W}}} - Q^f \frac{s^2_{\mathrm{W}}}{c_{\mathrm{W}}}\right) + \not{A}\left(s_{\mathrm{W}} Q^f\right)\right] f\,, \qquad \text{(C.1)}
$$

$$
\begin{aligned}
\mathcal{L}_b = -g \sum_b \left(b^\dagger \mathrm{i}\overset{\leftrightarrow}{\partial}_\mu b\right)&\left[Z^\mu\left(I_3^f \frac{1}{c_{\mathrm{W}}} - Q^f \frac{s^2_{\mathrm{W}}}{c_{\mathrm{W}}}\right)\right.\\
&\left.+A^\mu\left(s_{\mathrm{W}} Q^f\right)\right]. \qquad \text{(C.2)}
\end{aligned}
$$

The interaction Lagrangians are flavor-diagonal in the weak basis. In the mass basis, the interactions with the photon remain diagonal, because all mixed states A must have the same charge, Q_A. On the other hand, the interactions with the Z-boson, which depend on the charge (Q_A) and the third component of the weak isospin (I_{3A}), are not in general flavor-diagonal in the mass basis, because the mixed states may have different I_{3A} values.

For LFV processes, the interaction of the photon and Z-boson with the charginos, neutralinos and sfermion fields is needed. The Lagrangian for the corresponding weak-basis fields is easily written knowing the charges and the I_3 of these fields. After transformation from the weak basis to the mass basis, the following interaction Lagrangians are obtained:

$$
\begin{aligned}
\mathcal{L}_{\chi^-} = -g\overline{\tilde{\chi}^-_A}\not{Z}\left[(E^{\mathrm{L}(\chi^-)}_{AB} P_{\mathrm{L}} + E^{\mathrm{R}(\chi^-)}_{AB} P_{\mathrm{R}}) + \frac{s^2_{\mathrm{W}}}{c_{\mathrm{W}}}\delta_{BA}\right]\tilde{\chi}^-_B\\
+e\overline{\tilde{\chi}^-_A}\not{A}\delta_{AB}\tilde{\chi}^-_B\,, \qquad \text{(C.3)}
\end{aligned}
$$

$$
\mathcal{L}_{\chi^0} = -g\overline{\tilde{\chi}^0_A}\not{Z}\left[E^{\mathrm{L}(\chi^0)}_{AB} P_{\mathrm{L}} + E^{\mathrm{R}(\chi^0)}_{AB} P_{\mathrm{L}}\right]\tilde{\chi}^0_B\,, \qquad \text{(C.4)}
$$

$$
\mathcal{L}_{\tilde{f}} = -g\tilde{f}^*_X \mathrm{i}\overset{\leftrightarrow}{\partial}_\mu \tilde{f}_Y Z^\mu\,[D^{\tilde{f}}_{XY}] - e\tilde{f}^*_X \mathrm{i}\overset{\leftrightarrow}{\partial}_\mu \tilde{f}_Y A^\mu\,[Q^{\tilde{f}}]\,, \qquad \text{(C.5)}
$$

where

$$
E^{\mathrm{L}(\chi^-)}_{AB} = -\frac{1}{c_{\mathrm{W}}}\left((O_{\mathrm{L}})_{A1}(O^*_{\mathrm{L}})_{B1} + \frac{1}{2}(O_{\mathrm{L}})_{A2}(O^*_{\mathrm{L}})_{B2}\right), \qquad \text{(C.6)}
$$

$$
E^{\mathrm{R}(\chi^-)}_{AB} = -\frac{1}{c_{\mathrm{W}}}\left((O_{\mathrm{R}})_{A1}(O^*_{\mathrm{R}})_{B1} + \frac{1}{2}(O_{\mathrm{R}})_{A2}(O^*_{\mathrm{R}})_{B2}\right), \qquad \text{(C.7)}
$$

$$
E^{\mathrm{L}(\chi^0)}_{AB} = -\frac{1}{c_{\mathrm{W}}}\left(\frac{1}{2}(O_N)_{A3}(O^*_N)_{B3} - \frac{1}{2}(O_N)_{A4}(O^*_N)_{B4}\right), \qquad \text{(C.8)}
$$

$$
E^{\mathrm{R}(\chi^0)}_{AB} = -E^{\mathrm{L}(\chi^0)*}_{AB}, \qquad \text{(C.9)}
$$

$$
D^{\tilde{f}_{\mathrm{L}}}_{XY} = I_3^{\tilde{f}_{\mathrm{L}}}(U_{\tilde{f}})_{Xi}(U^*_{\tilde{f}})_{Yi} - Q_3^{\tilde{f}_{\mathrm{L}}}\frac{s^2_{\mathrm{W}}}{c_{\mathrm{W}}}. \qquad \text{(C.10)}
$$

Here, in the definition of $D^{\tilde{f}}_{XY}$, the index i is for summing over the generation 1, 2 and 3. $Q^{\tilde{f}_{\mathrm{L}}}$ is the charge of the sfermion $\tilde{f}_{\mathrm{L}}$, and $I_3^{\tilde{f}_{\mathrm{L}}}$ is its third component of isospin in the weak basis. The charges and third components of the isospin of the weak-basis fields for the charginos and neutralinos are explicitly written in the definitions of the constants $E^{\mathrm{L,R}(\chi^-)}_{AB}$ and $E^{\mathrm{L,R}(\chi^0)}_{AB}$.

Appendix D: Loop functions

In this appendix the loop functions appearing in the Z-boson amplitude and the box amplitudes are listed.

D.1 Z-boson loop functions

The Z-boson amplitude comprises two-loop functions from the triangle-diagram part of the amplitude, $F_1(a,b,c)$ and $F_2(a,b,c)$, and two-loop functions from the self-energy part of the amplitude, $f_1(a,b)$ and $f_2(a,b)$. These loop functions are

$$
F_1(a,b,c) = -\frac{1}{b-c}\left[\frac{a\ln a - b\ln b}{a-b} - \frac{a\ln a - c\ln c}{a-c}\right], \qquad \text{(D.1)}
$$

$$
\begin{aligned}
F_2(a,b,c) = \frac{3}{8} - \frac{1}{4}\frac{1}{b-c}&\\
\times\left[\frac{a^2\ln a - b^2\ln b}{a-b} - \frac{a^2\ln a - c^2\ln c}{a-c}\right]&, \qquad \text{(D.2)}
\end{aligned}
$$

$$
f_1(a,b) = \frac{1}{2} - \frac{\ln a}{2} + \frac{-a^2+b^2+2b^2(\ln a - \ln b)}{4(a-b)^2}\,, \qquad \text{(D.3)}
$$

$$
f_2(a,b) = \frac{1}{2} - \frac{\ln b}{2} + \frac{a^2-b^2+2a^2(\ln b - \ln a)}{4(a-b)^2}\,. \qquad \text{(D.4)}
$$

They are evaluated by neglecting the momenta of incoming and outgoing particles. The functions F_1 and F_2 are

symmetric with respect to the replacement of their arguments (a, b and c). In the limit of two equal arguments, the functions F_1 and F_2 have the following form:

$$F_1(a,b,b) = \frac{a-b-a\ln a+a\ln b}{(a-b)^2}\,, \tag{D.5}$$

$$F_2(a,b,b) = \frac{1}{4}-\frac{\ln b}{4}+\frac{a^2-b^2+2a^2(\ln b-\ln a)}{8(a-b)^2}\,. \tag{D.6}$$

The arguments of the logarithms appearing in the F_1 and F_2 can be divided by any constant, which can be used to redefine these functions as functions of two variables, for instance b/a and c/a. The troublesome $\ln b$ term in the f_2 function can be replaced with $\ln(b/a)$ because of the unitarity cancellations in the sum $N^{\mathrm{R}(e)}_{jBY}N^{\mathrm{R}(e)*}_{iAX}$, and therefore f_1 and f_2 can be expressed in terms of one variable (b/a) only.

D.2 Box-loop functions

The box amplitude contains two-loop functions, d_0 and d_2:

$$\begin{aligned} &d_0(x,y,z,w) = \\ &\quad\frac{x\ln x}{(y-x)(z-x)(w-x)}+\frac{y\ln y}{(x-y)(z-y)(w-y)} \\ &+\frac{z\ln z}{(x-z)(y-z)(w-z)}+\frac{w\ln w}{(x-w)(y-w)(z-w)}, \end{aligned} \tag{D.7}$$

$$\begin{aligned} &d_2(x,y,z,w) = \\ &\quad\frac{1}{4}\left\{\frac{x^2\ln x}{(y-x)(z-x)(w-x)}+\frac{y^2\ln y}{(x-y)(z-y)(w-y)}\right. \\ &\left.+\frac{z^2\ln z}{(x-z)(y-z)(w-z)}+\frac{w^2\ln w}{(x-w)(y-w)(z-w)}\right\}. \end{aligned} \tag{D.8}$$

As mentioned before, they are also by evaluated neglecting the momenta of the incoming and outgoing particles.

Appendix E: Meson states and quark currents

Meson states are assumed to contain valence quarks only. The quark–antiquark ($q_aq_b^c$) content of the pseudoscalar-meson states is given in the Table 2. The quark–antiquark content of the vector-meson states is obtained by replacing the fields K^+, K^0, π^+, π^0, π^-, $\bar{K}^0$ K^-, η_8, η_1, η and η' by the fields K^{*+}, K^{*0}, ρ^+, ρ^0, ρ^-, $\overline{K^{*0}}$, $\overline{K^{*-}}$, ϕ_8, ϕ_1, ϕ and ω, and the angle θ_P by the angle θ_V. From the quark content of the meson fields, one can find the meson content of e.g. the axial-vector (A) and vector (V) quark currents (factor of proportionality, Lorentz indices and spinor structures are neglected),

$$(\bar{u}u)_A \sim \left(\frac{c_P}{\sqrt{6}}-\frac{s_P}{\sqrt{3}}\right)\eta^\dagger+\left(\frac{s_P}{\sqrt{6}}+\frac{c_P}{\sqrt{3}}\right)\eta'^\dagger+\frac{1}{\sqrt{2}}\pi^{0\dagger}$$

Table 2. Quark content of the pseudoscalar-meson states and fields: the listed meson states correspond to the tensor description of meson states [45]. The shorthand notation $c_P=\cos\theta_P$ and $s_P=\sin\theta_P$ is used

$\lvert M\rangle$	Quark content of $\lvert M\rangle$	Quark content of $M(x)$
$\lvert K^+\rangle$	$us^c\sim b_u^\dagger d_s^\dagger$	$su^c\sim d_s b_u$
$\lvert K^0\rangle$	ds^c	sd^c
$\lvert\pi^+\rangle$	ud^c	du^c
$\lvert\pi^0\rangle$	$\frac{1}{\sqrt{2}}(uu^c-dd^c)$	$\frac{1}{\sqrt{2}}(uu^c-dd^c)$
$\lvert\pi^-\rangle$	du^c	ud^c
$\lvert K^-\rangle$	su^c	us^c
$\lvert\bar{K}^0\rangle$	sd^c	ds^c
$\lvert\eta_8\rangle$	$\frac{1}{\sqrt{6}}(uu^c+dd^c-2ss^c)$	$\frac{1}{\sqrt{6}}(uu^c+dd^c-2ss^c)$
$\lvert\eta_1\rangle$	$\frac{1}{\sqrt{6}}(uu^c+dd^c+ss^c)$	$\frac{1}{\sqrt{6}}(uu^c+dd^c+ss^c)$
$\lvert\eta\rangle$	$c_P\lvert\eta_8\rangle-s_P\lvert\eta_1\rangle$	$c_P\eta_8(x)-s_P\eta_1(x)$
$\lvert\eta'\rangle$	$s_P\lvert\eta_8\rangle+c_P\lvert\eta_1\rangle$	$s_P\eta_8(x)+c_P\eta_1(x)$

Table 3. Combinations of $k^{P,V}_{\bar{q}_aq_b}$ constants appearing in the photon-penguin a nd the Z-boson-penguin $\ell\to\ell' P(V)$ amplitudes

k	ρ^0	ϕ	ω
k^V_γ	$\frac{1}{\sqrt{2}}$	$\frac{1}{\sqrt{6}}c_V$	$\frac{1}{\sqrt{6}}s_V$
k^V_Z	$\frac{1}{\sqrt{2}}c_{2\mathrm{W}}$	$\frac{c_V}{\sqrt{6}}c_{2\mathrm{W}}+\frac{s_V}{2\sqrt{3}}$	$\frac{s_V}{\sqrt{6}}c_{2\mathrm{W}}-\frac{c_V}{2\sqrt{3}}$
k	π^0	η	η'
k^P_Z	$\frac{1}{\sqrt{2}}$	$\frac{c_P}{\sqrt{6}}+\frac{s_P}{2\sqrt{3}}$	$\frac{s_P}{\sqrt{6}}-\frac{c_P}{2\sqrt{3}}$

$$\begin{aligned} &\equiv k^\eta_{\bar{u}u}\eta^\dagger+k^{\eta'}_{\bar{u}u}\eta'^\dagger+k^{\pi^0}_{\bar{u}u}\pi^{0\dagger} \\ (\bar{d}d)_A &\sim \left(\frac{c_P}{\sqrt{6}}-\frac{s_P}{\sqrt{3}}\right)\eta^\dagger+\left(\frac{s_P}{\sqrt{6}}+\frac{c_P}{\sqrt{3}}\right)\eta'^\dagger-\frac{1}{\sqrt{2}}\rho^{0\dagger} \\ &\equiv k^\eta_{\bar{d}d}\eta^\dagger+k^{\eta'}_{\bar{d}d}\eta'^\dagger+k^{\pi^0}_{\bar{d}d}\pi^{0\dagger} \\ (\bar{s}s)_A &\sim \left(-\frac{2c_P}{\sqrt{6}}-\frac{s_P}{\sqrt{3}}\right)\eta^\dagger+\left(-\frac{2s_P}{\sqrt{6}}+\frac{c_P}{\sqrt{3}}\right)\eta'^\dagger \\ &\equiv k^\eta_{\bar{s}s}\eta^\dagger+k^{\eta'}_{\bar{s}s}\eta'^\dagger \end{aligned} \tag{E.1}$$

$$\begin{aligned} (\bar{u}u)_V &\sim \left(\frac{c_V}{\sqrt{6}}-\frac{s_V}{\sqrt{3}}\right)\phi^\dagger+\left(\frac{s_V}{\sqrt{6}}+\frac{c_V}{\sqrt{3}}\right)\omega^\dagger+\frac{1}{\sqrt{2}}\rho^{0\dagger} \\ &\equiv k^\phi_{\bar{u}u}\phi^\dagger+k^\omega_{\bar{u}u}\omega^\dagger+k^{\rho^0}_{\bar{u}u}\rho^{0\dagger} \\ (\bar{d}d)_V &\sim \left(\frac{c_V}{\sqrt{6}}-\frac{s_V}{\sqrt{3}}\right)\phi^\dagger+\left(\frac{s_V}{\sqrt{6}}+\frac{c_V}{\sqrt{3}}\right)\omega^\dagger-\frac{1}{\sqrt{2}}\rho^{0\dagger} \\ &\equiv k^\phi_{\bar{d}d}\phi^\dagger+k^\omega_{\bar{d}d}\omega^\dagger+k^{\rho^0}_{\bar{d}d}\rho^{0\dagger} \\ (\bar{s}s)_V &\sim \left(-\frac{2c_V}{\sqrt{6}}-\frac{s_V}{\sqrt{3}}\right)\phi^\dagger+\left(-\frac{2s_V}{\sqrt{6}}+\frac{c_V}{\sqrt{3}}\right)\omega^\dagger \\ &\equiv k^\phi_{\bar{s}s}\phi^\dagger+k^\omega_{\bar{s}s}\omega^\dagger\,. \end{aligned} \tag{E.2}$$

Here $s_V=\sin\theta_V$, and $c_V=\cos\theta_V$, and the numerical factors are normalizations of mesons expressed in terms of the quark fields. The combinations of constants $k^{P,V}_{\bar{q}_aq_b}$ are contained in the expressions for all quark currents (from the scalar-quark current to the tensor-quark current), and we

introduce them to abbreviate the expressions for the box form factors.

The photon-penguin and the Z-boson-penguin amplitudes contain the combinations of constants $k^{P,V}_{\bar{q}_a q_b}$ given in Table 3. For instance, $k^{\rho^0}_{\gamma} = Q_u k^{\rho_0}_{\bar{u}u} + Q_d k^{\rho_0}_{\bar{d}d} + Q_s k^{\rho_0}_{\bar{s}s}$.

References

1. SuperKamiokande Collaboration, Y. Fukuda et al., Phys. Rev. Lett. **81**, 1562 (1998)
2. Z. Maki, N. Nakagawa, S. Sakata, Prog. Theor. Phys. **28**, 870 (1962)
3. SNO Collaboration, Q.R. Ahmad et al., Phys. Rev. Lett. **89**, 011 301 (2002)
4. SNO Collaboration, Q.R. Ahmad et al., Phys. Rev. Lett. **89**, 011 302 (2002)
5. KamLAND Collaboration, K. Eguchi et al., Phys. Rev. Lett. **90**, 021 802 (2003)
6. F. Wilczek, A. Zee, Phys. Rev. Lett. **43**, 1571 (1979)
7. S. Weinberg, Phys. Rev. Lett. **43**, 1566 (1979)
8. H.A. Weldon, A. Zee, Nucl. Phys. B **173**, 269 (1980)
9. T.P. Cheng, L.F. Lee, T.P. Cheng, L.F. Lee, Phys. Rev. D **16**, 1425 (1977)
10. P. Minikowski, Phys. Lett. B **421**, 67 (1977)
11. J.D. Bjorken, K. Lane, S. Weinberg, Phys. Rev. D **16**, 1474 (1977)
12. G. Altarelli, L. Baulieu, N. Cabibbo, L. Maiani, R. Petronzio, Nucl. Phys. B **125**, 285 (1977)
13. T.P. Cheng, L.F. Lee, Phys. Rev. Lett. **45**, 1809 (1980)
14. E. Ma, A. Pramudita, Phys. Rev. D **24**, 1410 (1981)
15. S.T. Petcov, Phys. Lett. B **115**, 401 (1982)
16. T.K. Kuo, N. Nakagawa, Phys. Rev. D **32**, 306 (1985)
17. G.K. Leontaris, K. Tamvakis, J.D. Vergados, Phys. Lett. B **171**, 412 (1986)
18. F. Borzumati, A. Masiero, Phys. Rev. Lett. **57**, 961 (1986)
19. J. Bernabéu, A. Santamaria, J. Vidal, A. Mendez, J.W.F. Valle, Phys. Lett. B **187**, 303 (1987)
20. J.O. Eeg, Z. Phys. C **46**, 665 (1990)
21. R. Arnowitt, P. Nath, Phys. Rev. Lett. **66**, 2708 (1991)
22. M. Sher, Y. Yuan, Phys. Rev. D **44**, 1461 (1991)
23. M.C. Gonzalez-Garcia, J.W.F. Valle, Mod. Phys. Lett. A **7**, 477 (1992)
24. R.N. Mohapatra, Phys. Rev. D **46**, 2990 (1992)
25. J. Wu, S. Urano, R. Arnowitt, Phys. Rev. D **47**, 4006 (1993)
26. T.S. Kosmas, G.K. Leontaris, J.D. Vergados, Prog. Part. Nucl. Phys. **33**, 397 (1994), and references therein
27. R.N. Mohapatra, S. Nussinov, X. Zhang, Phys. Rev. D **49**, 2410 (1994)
28. D. Ng, J.N. Ng, Phys. Lett. B **331**, 371 (1994)
29. D. Tommasini, G. Barenboim, J. Bernabéu, C. Jarlskog, Nucl. Phys. B **444**, 451 (1995)
30. P. Depommier, C. Leroy, Rep. Prog. Phys. **58**, 61 (1995), and references therein
31. R. Barbieri, L.J. Hall, A. Strumia, Nucl. Phys. B **445**, 219 (1995) [arXiv:hep-ph/9501334]
32. G. Barenboim, M. Raidal, Nucl. Phys. B **484**, 63 (1997)
33. G. Couture, M. Frank, H. Konig, Eur. Phys. J. C **7**, 135 (1999)
34. R. Kitano, K. Yamamoto, arXiv:hep-ph/9710389
35. M. Raidal, A. Santamaria, Phys. Lett. B **421**, 250 (1998)
36. Y. Kuno, Y. Okada, Rev. Mod. Phys. **73**, 151 (2001) and references therein
37. T. Blažek, S.F. King, Nucl. Phys. B **662**, 359 (2003) [arXiv:hep-ph/0211368]
38. J.I. Illana, M. Masip, Eur. Phys. J. C **35**, 365 (2004)
39. F. Deppisch, J.W.F. Valle, Phys. Rev. D **72**, 036 001 (2005) [arXiv:hep-ph/0406040]
40. E.O. Iltan, JHEP **0408**, 020 (2004)
41. J. Hisano, Nucl. Phys. Proc. Suppl. **111**, 178 (2002) [arXiv:hep-ph/0204100],
42. A. Ilakovac, A. Pilaftsis, Nucl. Phys. B **437**, 491 (1995) [arXiv:hep-ph/9403398]
43. T. Fukuyama, T. Kikuchi, N. Okada, Phys. Rev. D **68**, 033 012 (2003) [arXiv:hep-ph/0304190]
44. A. Ilakovac, B.A. Kniehl, A. Pilaftsis, Phys. Rev. D **52**, 3993 (1995) [arXiv:hep-ph/9503456]
45. A. Ilakovac, Phys. Rev. D **54**, 5653 (1996) [arXiv:hep-ph/9608218]
46. S. Fajfer, A. Ilakovac, Phys. Rev. D **57**, 4219 (1998)
47. A. Ilakovac, Phys. Rev. D **62**, 036 010 (2000) [arXiv:hep-ph/9910213]
48. D. Black, T. Han, H.J. He, M. Sher, Phys. Rev. D **66**, 053 002 (2002) [arXiv:hep-ph/0206056]
49. M. Sher, Phys. Rev. D **66**, 057 301 (2002) [arXiv:hep-ph/0207136]
50. A. Brignole, A. Rossi, Nucl. Phys. B **701**, 3 (2004) [arXiv:hep-ph/0404211]
51. G. Farrar, P. Fayet, Phys. Lett. B **76**, 575 (1978)
52. C. Costa, F. Feruglio, F. Zwirner, Nuovo Cim. A **70**, 201 (1982)
53. F. Zwirner, Phys. Lett. B **132**, 103 (1983)
54. L. Hall, M. Suzuki, Nucl. Phys. B **231**, 419 (1985)
55. J. Ellis et al., Phys. Lett. B **150**, 142 (1985)
56. G. Ross, J. Valle, Phys. Lett. B **151**, 375 (1985)
57. S. Dawson, Nucl. Phys. B **261**, 297 (1985)
58. R. Barbieri, S. Ferrara, C.A. Savoy, Phys. Lett. B **119**, 343 (1982)
59. A.H. Chamseddine, R. Arnowitt, P. Nath, Phys. Rev. Lett. **49**, 970 (1982)
60. L.J. Hall, J. Lykken, S. Weinberg, Phys. Rev. D **27**, 2359 (1983)
61. M. Dine, A.E. Nelson, Phys. Rev. D **48**, 1277 (1993) [arXiv:hep-ph/9303230]
62. for a review, see, G.F. Giudice, R. Rattazzi, Phys. Rep. **322**, 419 (1999) [arXiv:hep-ph/9801271]
63. L. Randall, R. Sundrum, Nucl. Phys. B **557**, 79 (1999)
64. G.F. Giudice, M.A. Luty, H. Murayama, R. Rattazzi, JHEP **9812**, 027 (1998)
65. D.E. Kaplan, G.D. Kribs, M. Schmaltz, Phys. Rev. D **62**, 035 010 (2000)
66. Z. Chacko, M.A. Luty, A.E. Nelson, E. Ponton, JHEP **0001**, 003 (2000)
67. M. Schmaltz, W. Skiba, Phys. Rev. D **62**, 095 005 (2000)
68. Z. Chacko, M.A. Luty, JHEP **0105**, 067 (2001)
69. F. Borzumati, A. Masiero, Phys. Rev. Lett. **57**, 961 (1986)
70. J. Hisano, T. Moroi, K. Tobe, M. Yamaguchi, Phys. Rev. D **53**, 2442 (1996)
71. O. Igonkina, Experimental Status of tau LFV decays, Second Workshop on Discovery potential of an Asymmetric B Factory at 10^{36} Luminosity, 24 October 2003
72. D.B. MacFarlane, B Physics at a Super B Factory, DESY Tuesday seminars, 10 November 2004

73. N. Sato, Tau Physics at the Super B-Factory, Tau Physics at the Super B-Factory, Super B-Factory Workshop in Hawaii
74. T. Yanagida, in: Proc. Workshop on the Unified Theory and Baryon Number in the Universe, ed. by O. Sawada, A. Sugamoto (KEK, Tsukuba, 1979)
75. M. Gell-Mann, P. Ramond, R. Slansky, In: Supergravity, ed. by D. Freedman, P. van Nieuwenhuizen (North-Holland, Amsterdam, 1979)
76. R.N. Mohapatra, G. Senjanović, Phys. Rev. Lett. **44**, 912 (1980)
77. K.S. Babu, R.N. Mohapatra, Phys. Rev. Lett. **70**, 2845 (1993) [arXiv:hep-ph/9209215]
78. T. Fukuyama, N. Okada, JHEP **0211**, 011 (2002) [arXiv:hep-ph/0205066]
79. K. Matsuda, Y. Koide, T. Fukuyama, H. Nishiura, Phys. Rev. D **65**, 033 008 (2002)
80. K. Matsuda, Y. Koide, T. Fukuyama, H. Nishiura, Phys. Rev. D **65**, 079 904 (2002) [Erratum]
81. K. Matsuda, Y. Koide, T. Fukuyama, Phys. Rev. D **64**, 053 015 (2001)
82. K. Matsuda, T. Fukuyama, H. Nishiura, Phys. Rev. D **61**, 053 001 (2000)
83. H.S. Goh, R.N. Mohapatra, S.P. Ng, Phys. Lett. B **570**, 215 (2003) [arXiv:hep-ph/0303055]
84. H.S. Goh, R.N. Mohapatra, S.P. Ng, Phys. Rev. D **68**, 115 008 (2003) [arXiv:hep-ph/0308197]
85. B. Bajc, G. Senjanović, F. Vissani, Phys. Rev. Lett. **90**, 051 802 (2003) [arXiv:hep-ph/0210207]
86. B. Dutta, Y. Mimura, R.N. Mohapatra, Phys. Rev. D **69**, 115 014 (2004) [arXiv:hep-ph/0402113]
87. K. Matsuda, Phys. Rev. D **69**, 113 006 (2004) [arXiv:hep-ph/0401154]
88. T. Fukuyama, A. Ilakovac, T. Kikuchi, S. Meljanac, N. Okada, J. Math. Phys. **46**, 033 505 (2005) [arXiv:hep-ph/0405300]
89. T. Fukuyama, A. Ilakovac, T. Kikuchi, S. Meljanac, N. Okada, Eur. Phys. J. C **42**, 191 (2005) [arXiv:hep-ph/0401213]
90. T. Fukuyama, A. Ilakovac, T. Kikuchi, S. Meljanac, N. Okada, Phys. Rev. D **72**, 051 701 (2005) [arXiv:hep-ph/0412348]
91. T. Fukuyama, T. Kikuchi, N. Okada, Int. J. Mod. Phys. A **19**, 4825 (2004) [arXiv:hep-ph/0306025]
92. T. Fukuyama, A. Ilakovac, T. Kikuchi, S. Meljanac, N. Okada, JHEP **0409**, 052 (2004) [arXiv:hep-ph/0406068]
93. L.E. Ibáñez, C. Lopez, Nucl. Phys. B **233**, 511 (1984)
94. G.L. Kane, C. Kolda, L. Roszkowski, J.D. Wells, Phys. Rev. D **40**, 6173 (1994)
95. K. Inoue, A. Kakuto, H. Komatsu, S. Takeshita, Prog. Theor. Phys. **68**, 927 (1982)
96. L. Ibañez, G.G. Ross, Phys. Lett. B **110**, 215 (1982)
97. L. Alvarez-Gaume, M. Claudson, M.B. Wise, Nucl. Phys. B **207**, 96 (1982)
98. L. Alvarez-Gaume, J. Polchinski, M.B. Wise, Nucl. Phys. B **221**, 495 (1983)
99. H.P. Nilles, Phys. Rep. **110**, 1 (1984)
100. J. Hisano, T. Moroi, K. Tobe, M. Yamaguchi, Phys. Lett. B **327**, 579 (1995)
101. L.J. Hall, L. Randall, Phys. Rev. Lett. **65**, 2939 (1990)
102. S.P. Martin, In: Perspectives on Supersupermmetry, ed. by G.L. Kane (World Scientific, Singapore, 1997), p. 1
103. S.P. Martin, M.T. Vaughn, Phys. Rev. D **50**, 2282 (1994) [arXiv:hep-ph/9311340]
104. S.T. Petcov, S. Profumo, Y. Takanishi, C.E. Yaguna, Nucl. Phys. B **676**, 453 (2004) [arXiv:hep-ph/0306195]
105. R.E. Marshak, Riazuddin, C.P. Ryan, Weak Interactions in Particle Physics (Wiley, New York, 1969)
106. J.J. Sakurai, Currents and Mesons (University of Chicago Press, Chicago, 1969)
107. V. de Alfaro, S. Fubini, C. Rossetti, Currents in Hadron Physics (North-Holland, Amsterdam, 1973)
108. M. Zielinski, Acta Phys. Pol. B **18**, 455 (1987)
109. W.A. Bardeen, A.J. Buras, J.M. Gerard, Nucl. Phys. B **293**, 787 (1987)
110. W.A. Bardeen, A.J. Buras, J.M. Gerard, Phys. Lett. B **180**, 133 (1986)
111. R.S. Chivukula, J.M. Flynn, H. Georgi, Phys. Lett. B **171**, 453 (1986)
112. J. Gasser, H. Leutwyler, Ann. Phys. **158**, 142 (1984)
113. Particle Data Group, S. Eidelman et al., Phys. Lett. B **592**, 1 (2004)
114. M. Bando, T. Kugo, K. Yamawaki, Phys. Rep. **164**, 217 (1988)
115. M. Bando, T. Kugo, K. Yamawaki, Nucl. Phys. B **259**, 493 (1985)
116. H. Fusaoka, Y. Koide, Phys. Rev. D **57**, 3986 (1998) [arXiv:hep-ph/9712201]
117. P.H. Chankowski, Z. Pluciennik, Phys. Lett. B **316**, 312 (1993) [arXiv:hep-ph/9306333]
118. K.S. Babu, C.N. Leung, J. Pantaleone, Phys. Lett. B **319**, 191 (1993) [arXiv:hep-ph/9309223]
119. S. Antusch, M. Dress, J. Kersten, M. Lindner, M. Ratz, Phys. Lett. B **519**, 238 (2001) [arXiv:hep-ph/0108005]
120. S. Antusch, M. Dress, J. Kersten, M. Lindner, M. Ratz, Phys. Lett. B **525**, 130 (2002) [arXiv:hep-ph/0110366]
121. Belle Collaboration, Y. Enari, Phys. Lett. B **622**, 218 (2005)
122. Belle Collaboration, Y. Enari, Nucl. Phys. B Proc. Suppl. **144**, 173 (2005), talk given at "The 8th International Workshop on Tau-Lepton Physics (Tau04)", [http://www.hepl.phys.nagoya-u.ac.jp/public/Tau04/]
123. Belle Collaboration, Y. Yusa, Nucl. Phys. B Proc. Suppl. **144**, 161 (2005), talk given at "The 8th International Workshop on Tau-Lepton Physics (Tau04)", [http://www.hepl.phys.nagoya-u.ac.jp/public/Tau04/]
124. BaBar Collaboration, B. Aubert et al., arXiv:hep-ex/0508012
125. BaBar Collaboration, B. Aubert et al., Phys. Rev. Lett. **92**, 0 251 802 (2004)
126. BaBar Collaboration, M. Roney, Nucl. Phys. B Proc. Suppl. **144**, 155 (2005), talk given at "The 8th International Workshop on Tau-Lepton Physics (Tau04)", [http://www.hepl.phys.nagoya-u.ac.jp/public/Tau04/]
127. C.L. Bennett et al., Astrophys. J. Suppl. **148**, 1 (2003) [arXiv:astro-ph/0302207]
128. WMAP Collaboration, D.N. Spergel et al., Astrophys. J. Suppl. **148**, 175 (2003) [arXiv:astro-ph/0302209]
129. J. Ellis, K.A. Olive, Y. Santoso, V.C. Spanos, Phys. Lett. B **565**, 176 (2003) [arXiv:hep-ph/0303043]
130. A.B. Lahanas, D.V. Nanopoulos, Phys. Lett. B **568**, 55 (2003) [arXiv:hep-ph/0303130]
131. Muon g-2 Collaboration, G.W. Bennett et al., Phys. Rev. Lett. **92**, 161 802 (2004) [arXiv:hep-ex/0401008]
132. SuperKEKB Physics Working Group Collaboration, A.G. Akeroyd et al., arXiv:hep-ex/0406071